

MINISTÉRIO DA CIÊNCIA, TECNOLOGIA, INOVAÇÕES E COMUNICAÇÕES
INSTITUTO NACIONAL DE PESQUISAS ESPACIAIS

Cosmo-ufes
Center for Astrophysics and Cosmology

21st century & 21 cm cosmology

VERÃO QUÂNTICO 2021

Carlos Alexandre Wuensche

Divisão de Astrofísica - INPE

Plan of the lectures

- 21 cm cosmology
- **21 cm observations**
- the BINGO project

Introduction

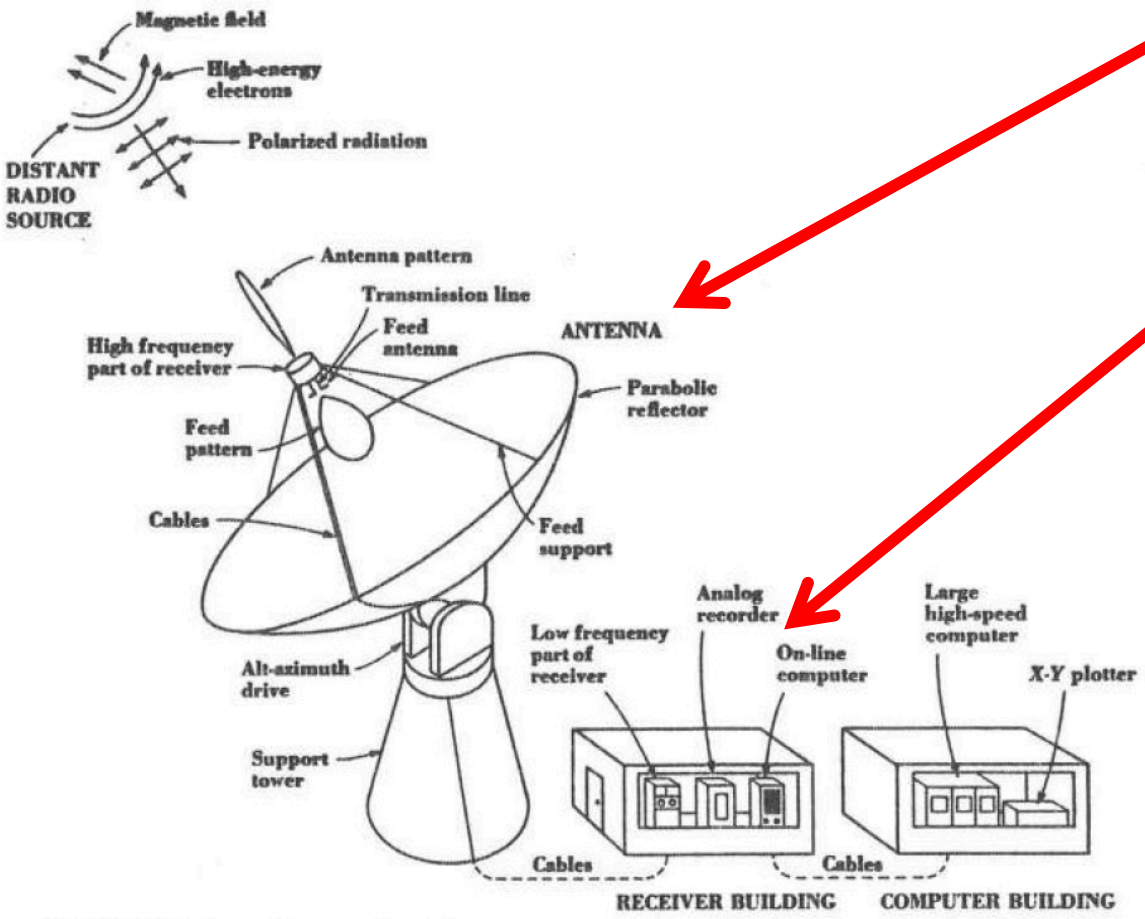
- 21 cm correspond to a radio band wavelength
- Its intensity reaches Earth radiotelescopes as a combination of signals from a huge volume in the Universe
- Nevertheless, sources emitting at different redshifts will reach Earth with different observing frequencies, compressing a tomographic signal into the observed frequency band
  - Galactic emission (mostly synchrotron)
  - Point radio sources (resolved)
  - Radio background (unresolved radio sources)
  - Man-made radio signals

- HI emission

At z=0 → λ = 21.106 cm (1420.405 MHz)
At z=0.01 → λ = 21.317 cm (1406.342 MHz)
At z=0.5 → λ = 31.659 cm (946.937 MHz)
At z=1 → λ = 42.212 cm (710.202 MHz)
At z=5 → λ = 42.212 cm (710.202 MHz)
At z=17 → λ = 3.799 **m** (78.911 MHz)

EDGES observation of a 21 cm absorption feature, when **t=220 Myr**

How does a radio telescope work?



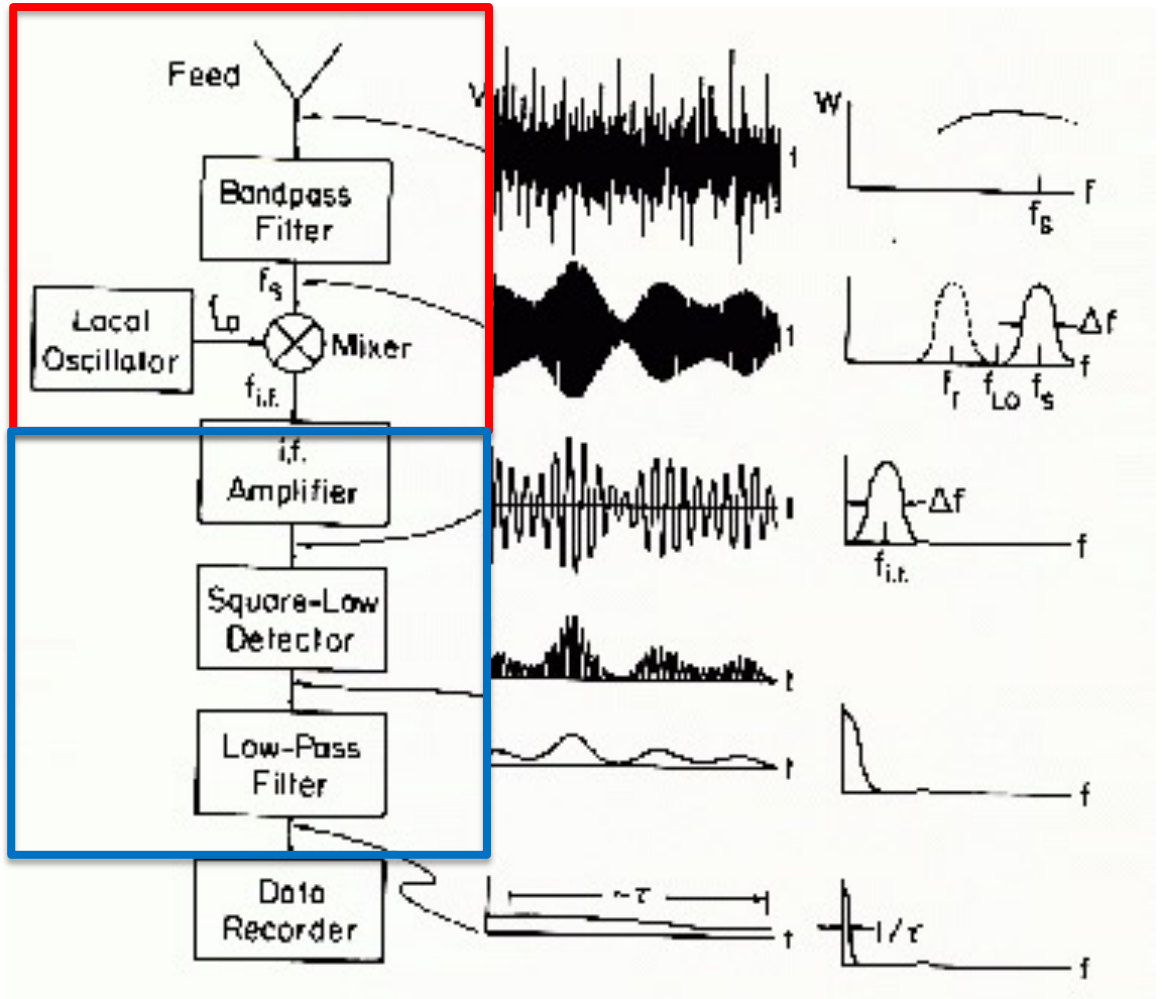


Source: Radio Astronomy (J. Kraus), cap.1

A more realistic system

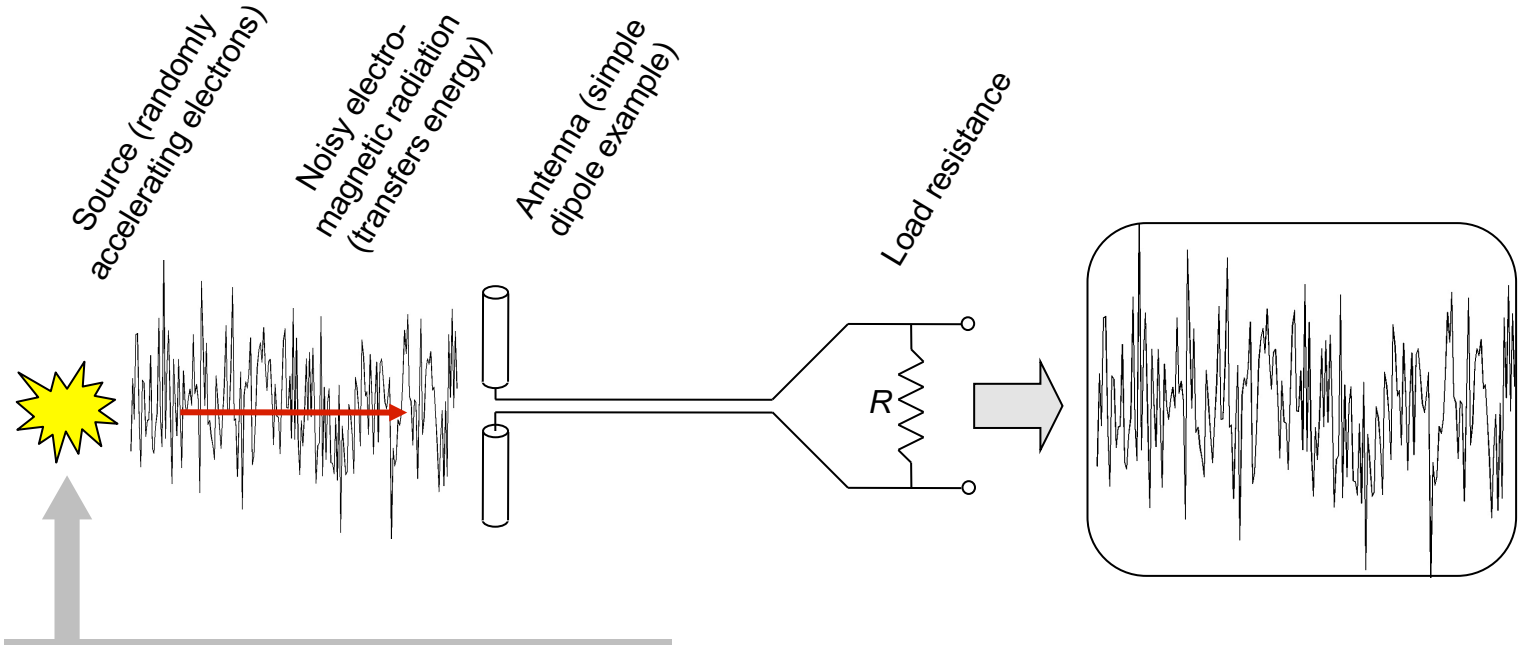
"Front end"

"Back end"



R M Price, "Radiometer Fundamentals", Meth. Exp. Phys. 12B (1976), Fig 1, section 3.1.4.

Noise and other Fundamentals



Types of electron acceleration:
- Thermal (random jiggling)
- Synchrotron (spiral)
- Spectral line (resonant sloshing)

Noise power spectrum

- Analyse the signal into Fourier components. *j*th component is:

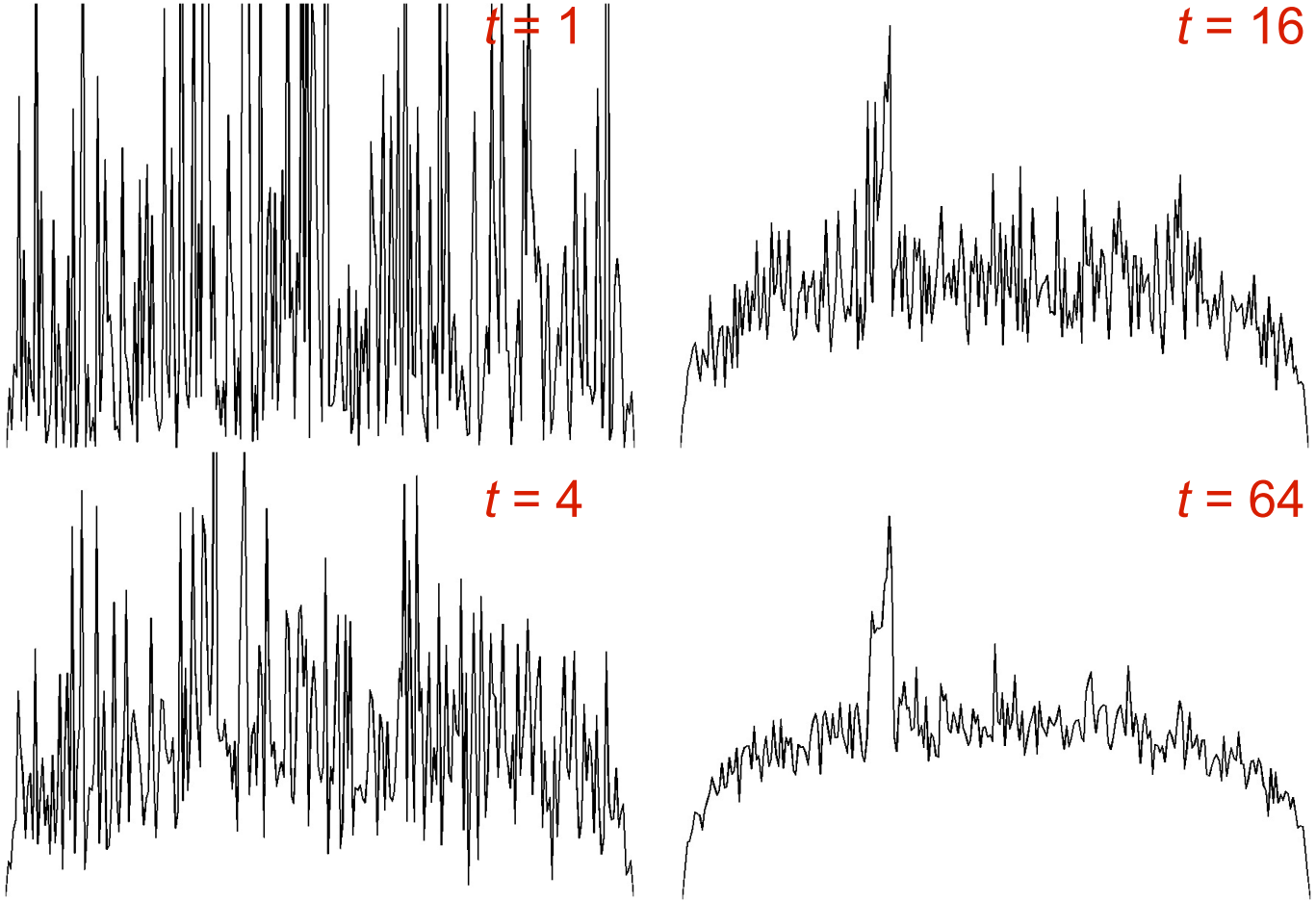
$$V_j(t) = V_j \exp(-i\omega_j t)$$
$$= V_j (\cos[\omega_j t] + i \sin[\omega_j t])$$

- The Fourier coefficient V_j is in general complex-valued. Power in this component is:

$$P_j = V_j^*(t) V_j(t)/R$$
$$= V_j^* V_j/R \, (\cos^2[\omega_j t] + \sin^2[\omega_j t])$$
$$= V_j^* V_j/R$$

- Closely related to the 'power spectrum' we've already encountered in Fourier theory.

Averaging the power spectrum



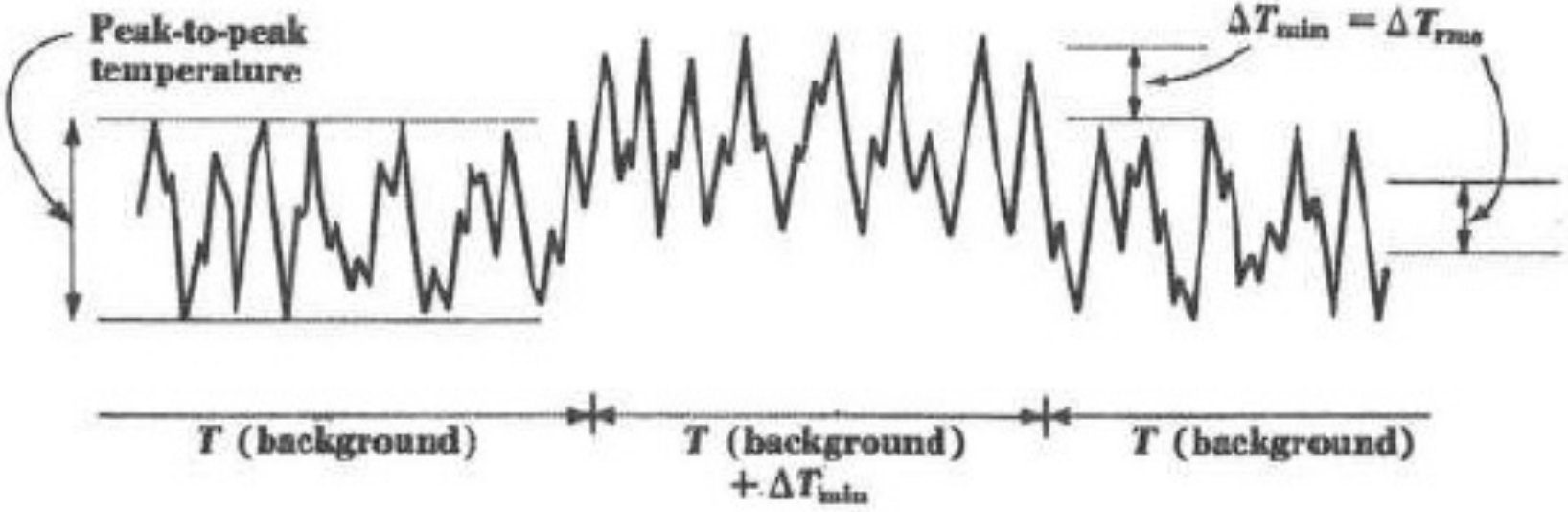
- The sensitivity, or minimum detectable temperature, of a radio telescope is equal to the rms noise temperature of the system as given by

$$\Delta T_{min} = \frac{K_{rec} T_{sys}}{\sqrt{\Delta \nu t_{obs}}} = \Delta T_{rms}$$

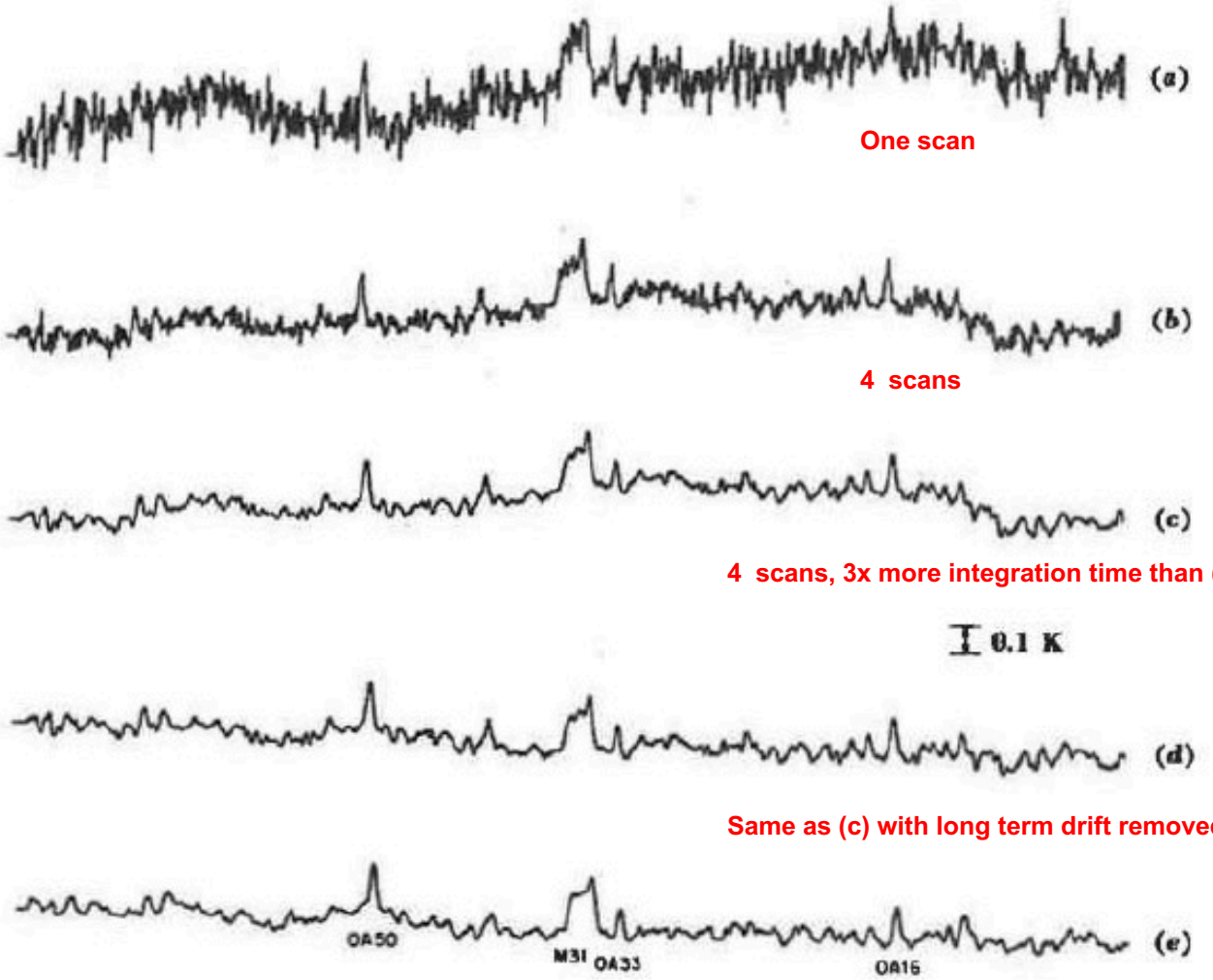
- ☑ ΔT_{min} = sensitivity, or minimum detectable temperature, K
- ☑ ΔT_{rms} = rms system noise temperature, K
- ☑ $T_{sys} = T_a + T_{LP}[(1/e) - 1] + (1/e)T_R$ = system noise temperature (at antenna terminals), K
- ☑ T_a = antenna noise temperature, K
- ☑ T_R = receiver noise temperature, K
- ☑ T_{LP} = physical temperature of transmission line (coaxial line or wave guide) between antenna and receiver, K
- ☑ e = transmission-line efficiency, dimensionless (0 <e < 1, =0.5 for 3dB atten.)
- ☑ K_{rec} = sensitivity constant, dimensionless
- ☑ Δv= predetection bandwidth, Hz
- ☑ t_{obs} = total integration time, sec

$$\Delta B_{min} = \frac{2k}{\lambda^2} \frac{K_{rec} T_{sys}}{\sqrt{\delta \nu t_{obs}}}$$

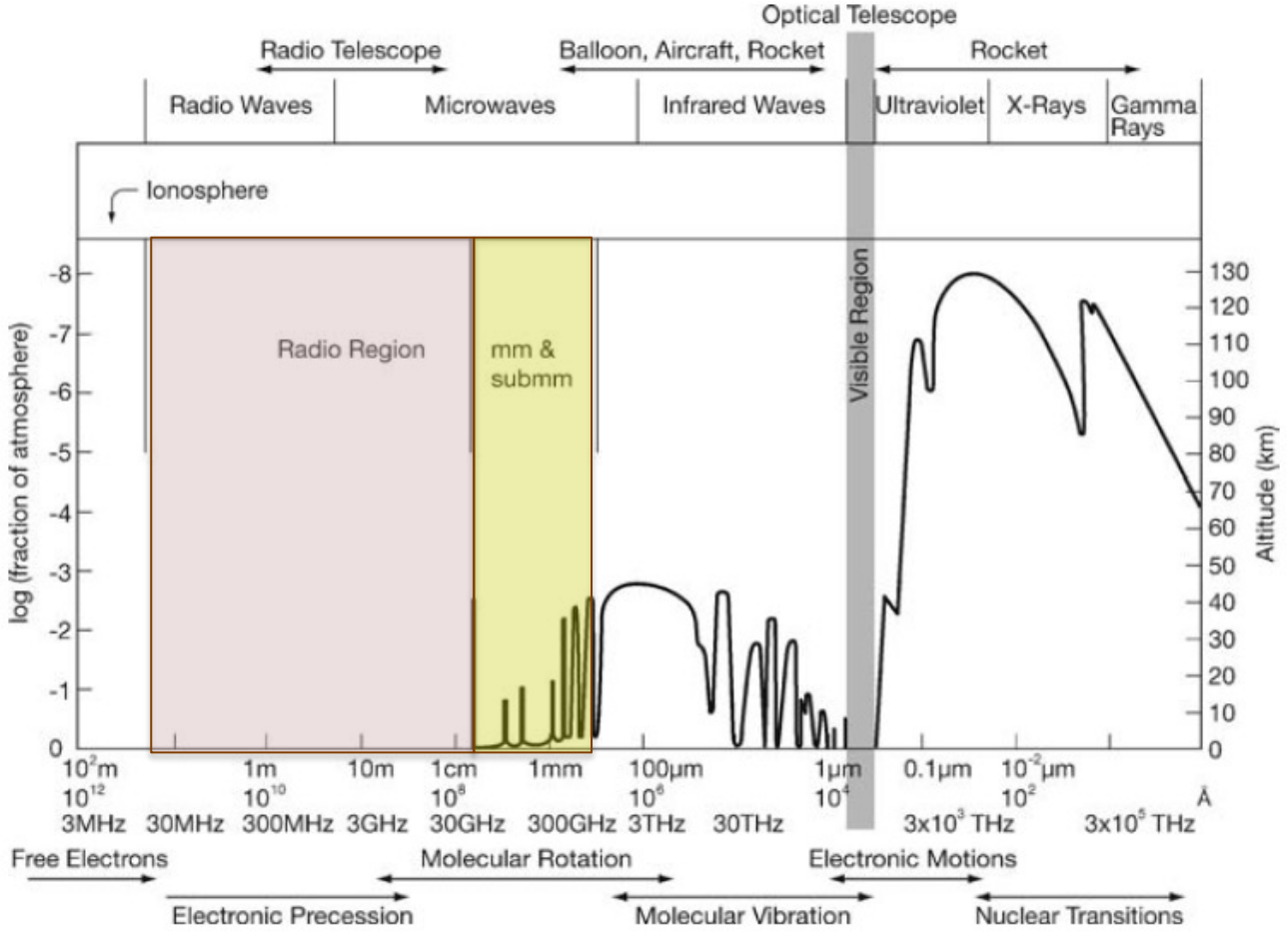
$$\Delta S_{min} = \frac{2k}{A_e} \frac{K_{rec} T_{sys}}{\sqrt{\delta \nu t_{obs}}}$$



Source: Radio Astronomy (J. Kraus) 1986


(a)
One scan
(b)
4 scans
(c)
4 scans, 3x more integration time than (b)
0.1 K
(d)
Same as (c) with long term drift removed
0A50
M31
0A33
0A16
(e)
11 scans, larger integration time and long term drift removed

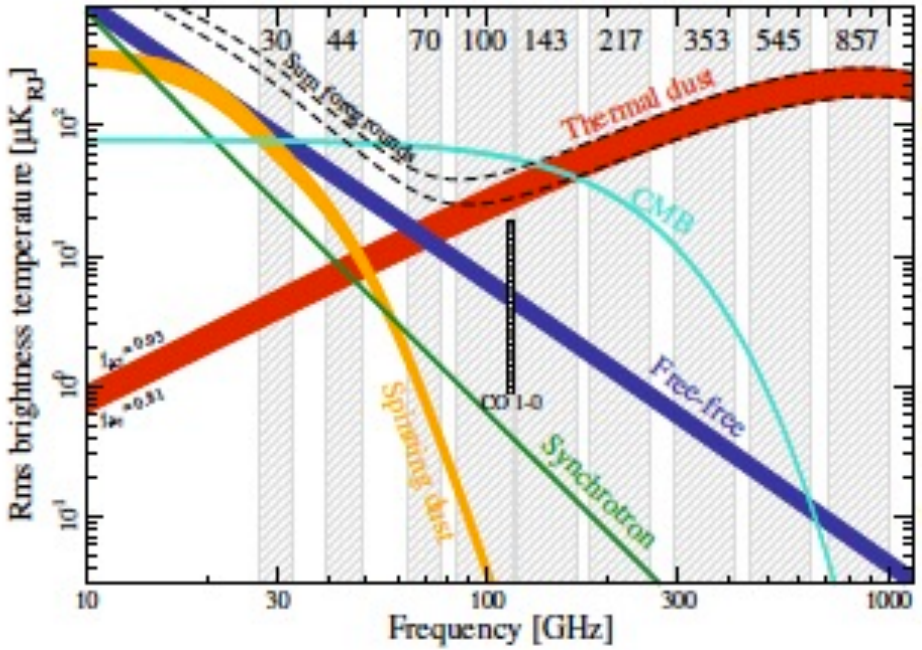
The atmospheric window

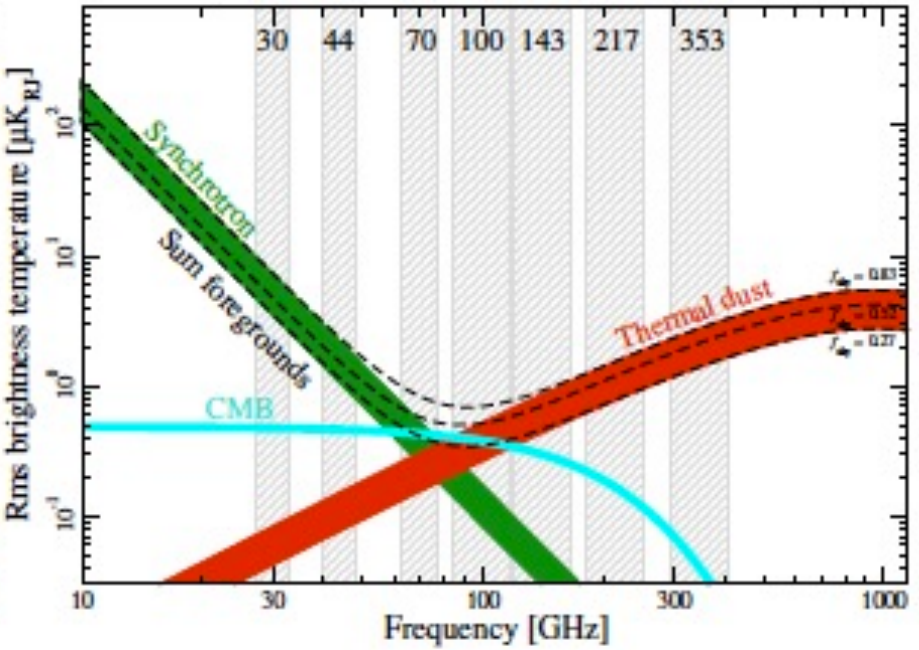


Credit: Wikipedia.org

C. A. Wuensche (2021)

The Galactic contribution



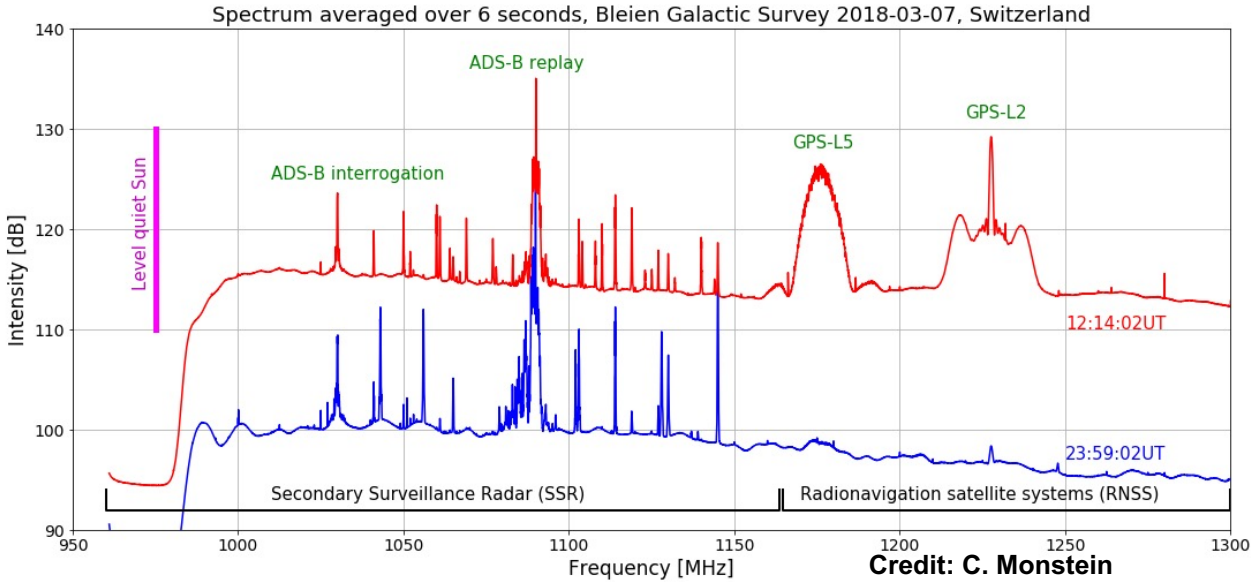


Credit: lambda.gsfc.nasa.gov

C. A. Wuensche (2021)

Radio Frequency Interference (RFI)

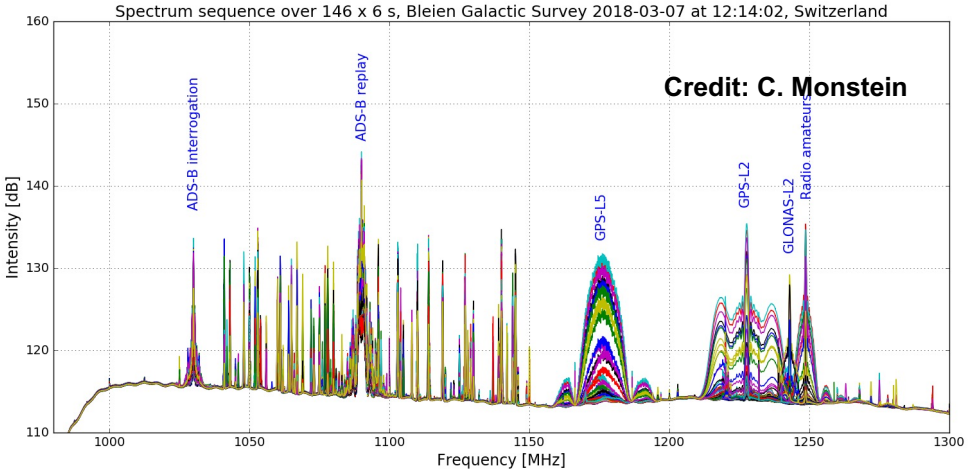
- RFI sources are man-made, and include active emitters (cellular phones and antennas, Wi-Fi networks, self-operating services such as house gates, satellites) and passive, unintentional emitters such as computers and car electronics.
- Some RFI sources can be partially removed, but their presence will always compromise the usefulness/efficiency of the astronomical data acquisition process.

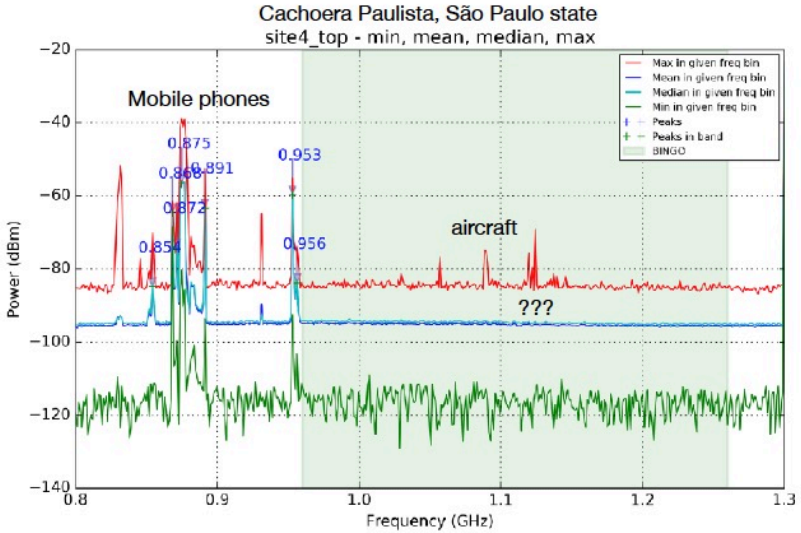


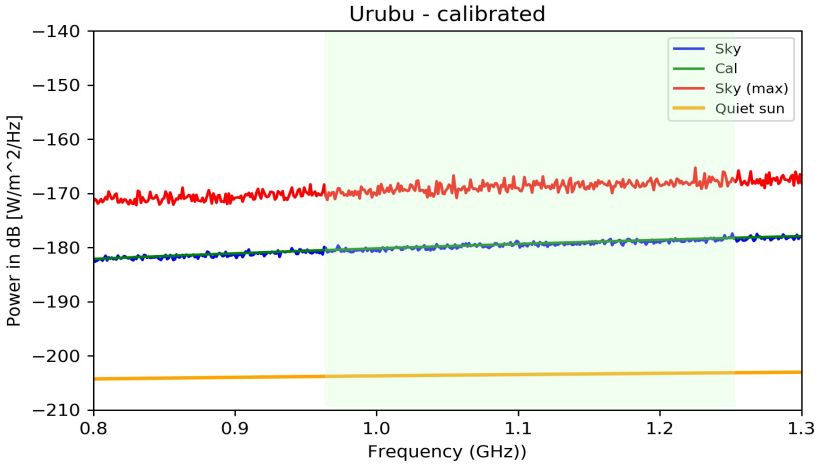
Credit: C. Monstein

C. A. Wuensche (2021)

RFI


Spectrum sequence over 146 x 6 s, Bleien Galactic Survey 2018-03-07 at 12:14:02, Switzerland
Credit: C. Monstein
ADS-B interrogation
ADS-B replay
GPS-L5
GPS-L2
GLONAS-L2
Radio amateur
Intensity [dB]
Frequency [MHz]


Cachoera Paulista, São Paulo state
site4_top - min, mean, median, max
Mobile phones
aircraft
???
0.875
0.868
0.891
0.953
0.872
0.854
0.956
Power (dBm)
Frequency (GHz)

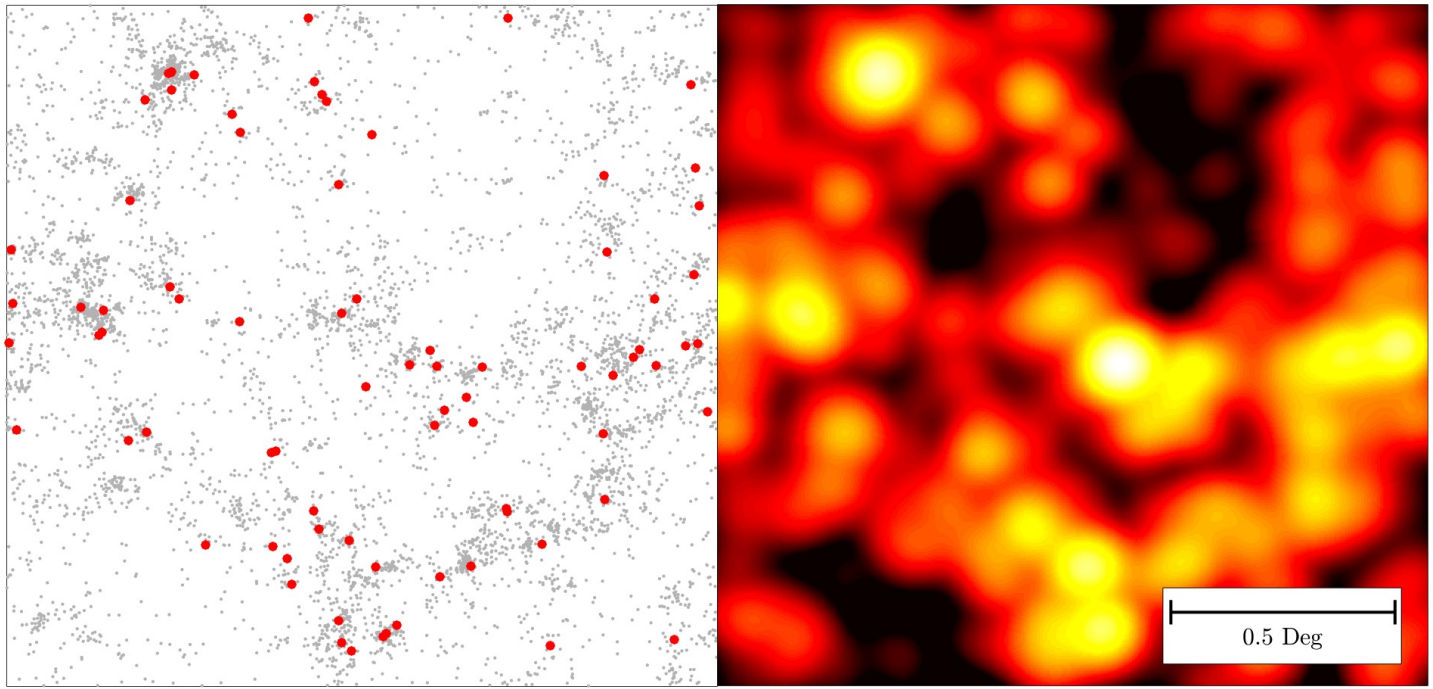

Urubu - calibrated
Sky
Cal
Sky (max)
Quiet sun
Power in dB [W/m^2/Hz]
Frequency (GHz))

Intensity mapping

The Intensity Mapping (IM) concept

Measure the large scale features from the integrated emission of galaxies + IGM, from spectral line of different elements (H, C, O, …), not worrying about individual objects

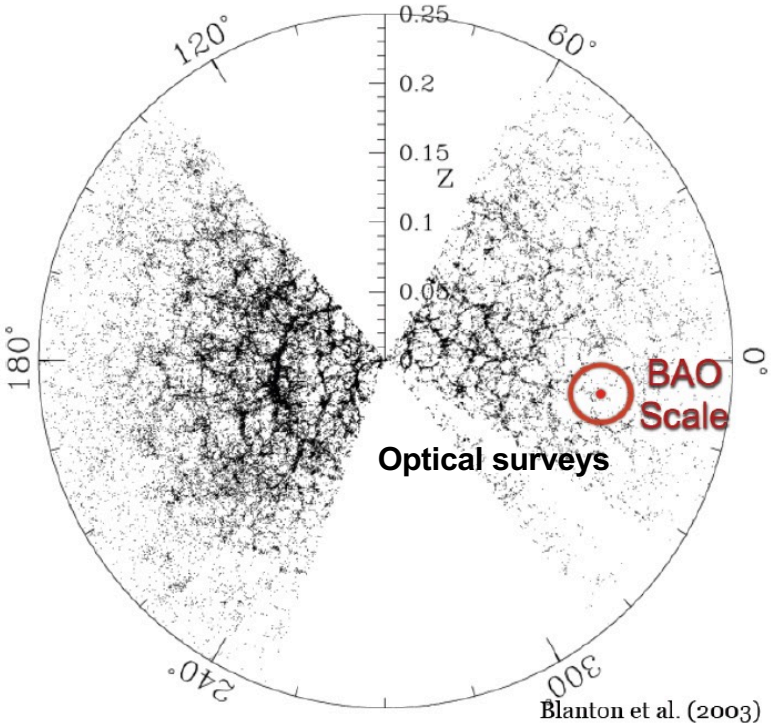
CO emission



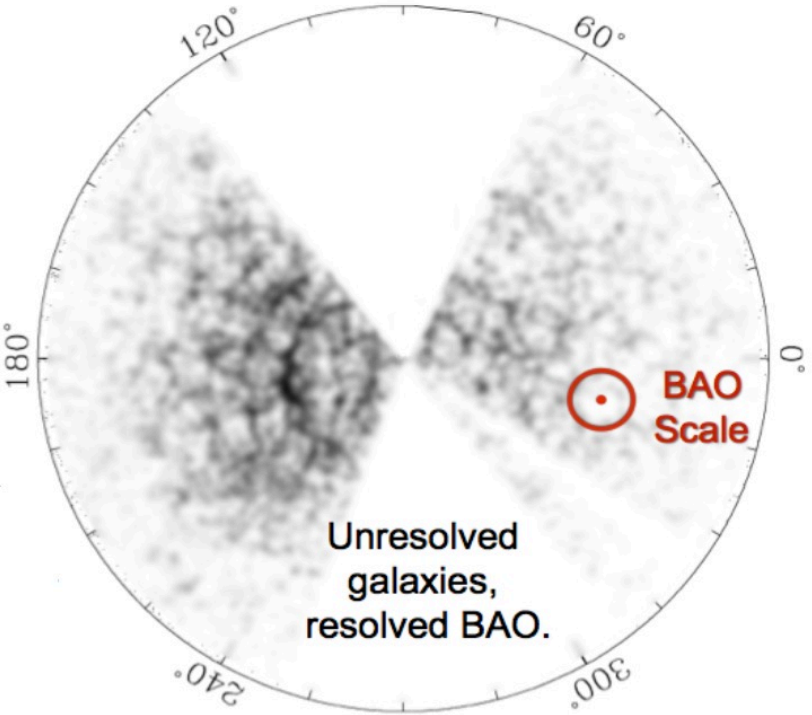
VLA (simulated, 4500h, detects 1% of all emitting sources in the FoV)

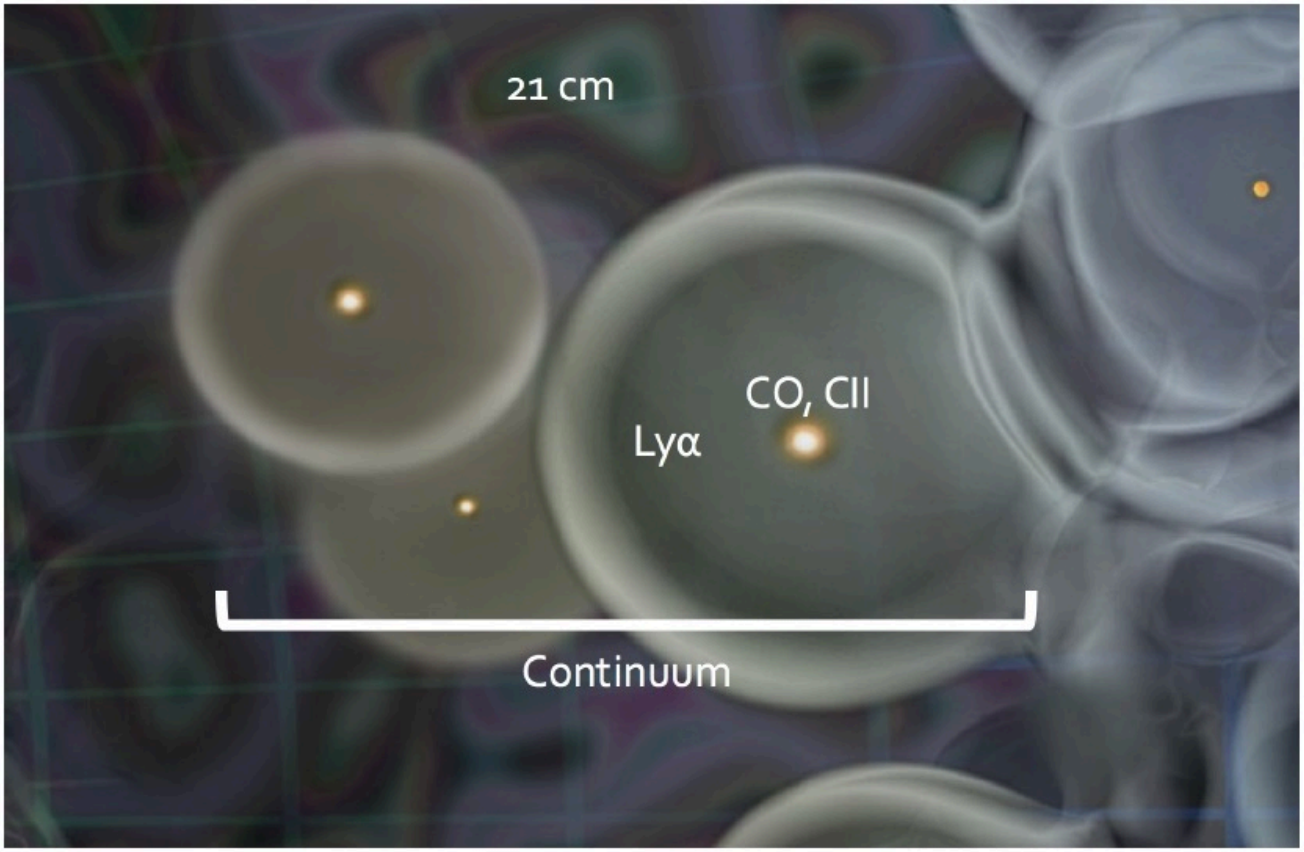
COMAP (simulated, 1500h, sensitive to all sources emitting in the FoV)

Kovetz et al, (arXiv:1709.09066)



Blanton et al. (2003)





CO, CII – star formation regions
Ly-alpha – galaxy halos
HI – neutral gas from outside bubbles
Continuum - CIB

Kovetz et al, (arXiv:1709.09066)

Different environments, different physics, deeper understanding of the star formation process at high-z

C. A. Wuensche (2021)

IM Formalism

Matter power spectrum

Shot noise power spectrum

$$P_k(z) = < I(z) >^2 \; b^2(z) \; P_m(k,z) + P_{shot}(z)$$

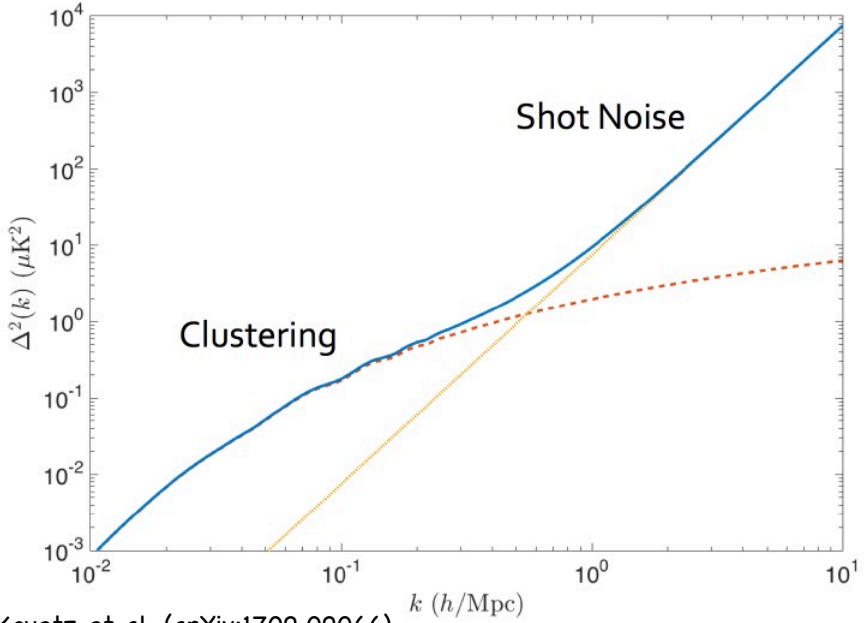
bias

$$< I(z) > \; \propto \; \int_0^\infty L\Phi(L,z)dL$$

$$P_{shot}(z) \; \propto \; \int_0^\infty L^2\Phi(L,z)dL$$

$$\Phi(L,z) \equiv dn(z)/dL$$

Line luminosity function



Kovetz et al, (arXiv:1709.09066)

$P_k(z)$ of the target emission line is determined by the astrophysical processes that take place in galaxies at different z

C. A. Wuensche (2021)

Line IM highlights

- Uses the integrated emission from spectral lines in galaxies and/or diffuse IGM to track growth and evolution of cosmic structure
- Covers very large volumes in a smaller amount of time, compared to optical surveys
- Reduced angular resolutions also allows for a wider instantaneous FOV
- Measure spatial fluctuations of the integrated flux of many unresolved objects instead of tracking one by one
- Sensitive to all objects emitting in that line, instead of being flux-limited
- Frequency of line emission directly relates to the z
- Besides HI, we can also investigate Hα, CO, C[II], Ly-α and OII

Line IM challenges

- Disentanglement of galactic and radio source emission, much stronger than the IM signal
- Confusion from interloping emission lines
- Non-gaussian nature of the signal
- Calibration uncertainties can significantly hamper the signal of interest
  - RFI interference
  - Beam calibration
    - many individual dishes and one beam for each dish
    - many beams illuminating a single dish
  - Receiver stability & gain fluctuations

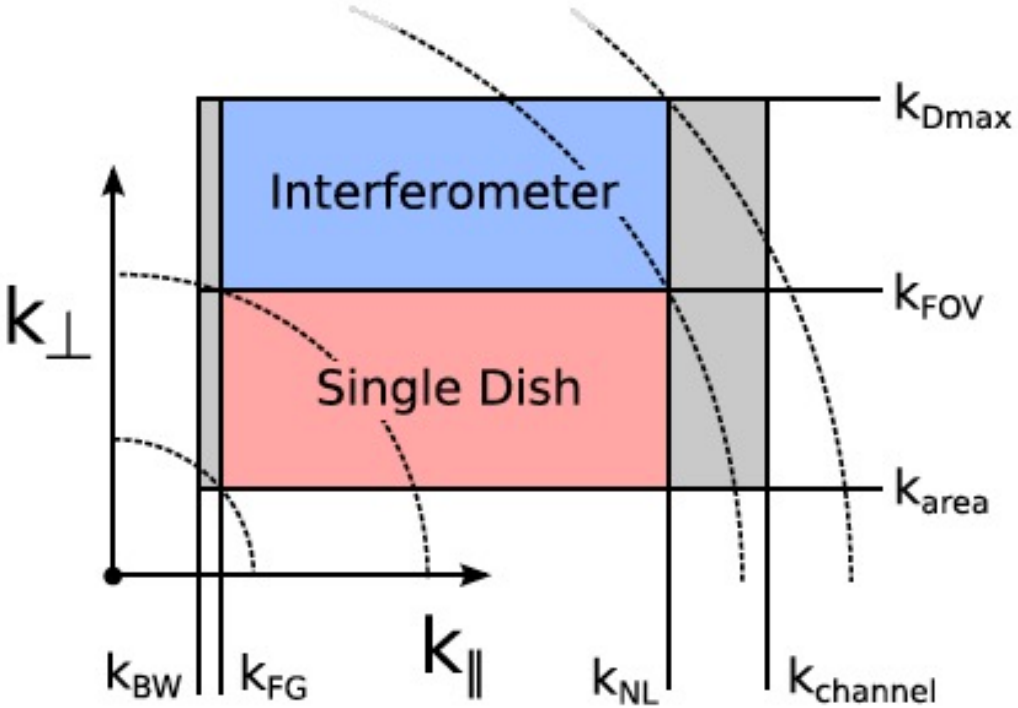
INSTRUMENTATION TO MEASURE THE 21cm LINE

Desirable items for a single dish HI surveyor

- Large collecting area (> 500 m^2)
- Large covered area on the sky (care should be taken with leaving out very small scales, < 0.1 $Mpc.h^{-1}$)
- Low sidelobes and good (precise shape) beam
- Long observing time (> 1 year)
- Sensitivity to intermediate scales, where BAO is important (0 < z < 2)
- Redshift range: 0.1 < z < 1 (bias larger than 0.7 after that)
- Frequency range:
  - 1300 MHz => z≈0.08
  - 100 MHz => z≈0.93

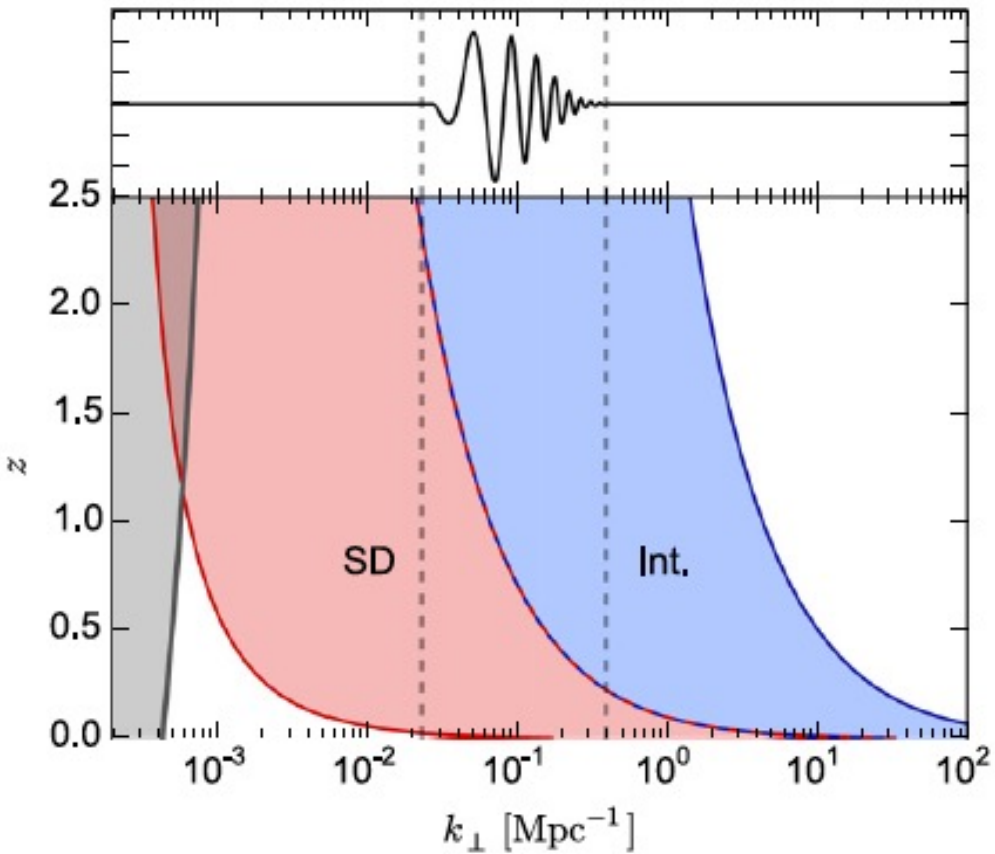
Lots of Radio Frequency Interference (RFI) in this frequency range

Adapted from Bull et al. 2015



$$k_\parallel^{\min} \sim k_{\rm FG} = 2\pi/\left(r_\nu \Delta\tilde{\nu}_{\rm tot}\right)$$
$$k_\parallel^{\max} \sim k_{\rm NL} = 1/\sigma_{\rm NL}$$
$$k_\perp^{\min} \sim k_{\rm area} = 2\pi/\sqrt{r^2 S_{\rm area}} \quad \text{(single dish)}$$
$$\sim k_{D_{\rm min}} = 2\pi D_{\rm min}/r\lambda \quad \text{(interferom.)}$$
$$k_\perp^{\max} \sim k_{\rm FOV} = 2\pi D_{\rm dish}/r\lambda \quad \text{(single dish)}$$
$$\sim k_{D_{\rm max}} = 2\pi D_{\rm max}/r\lambda \quad \text{(interferom.)}.$$

Bull et al. (ApJ 2015)



Bull et al. (ApJ 2015)

$$k_\parallel^{\min} \sim k_{\rm FG} = 2\pi/\left(r_\nu \Delta\tilde{\nu}_{\rm tot}\right)$$

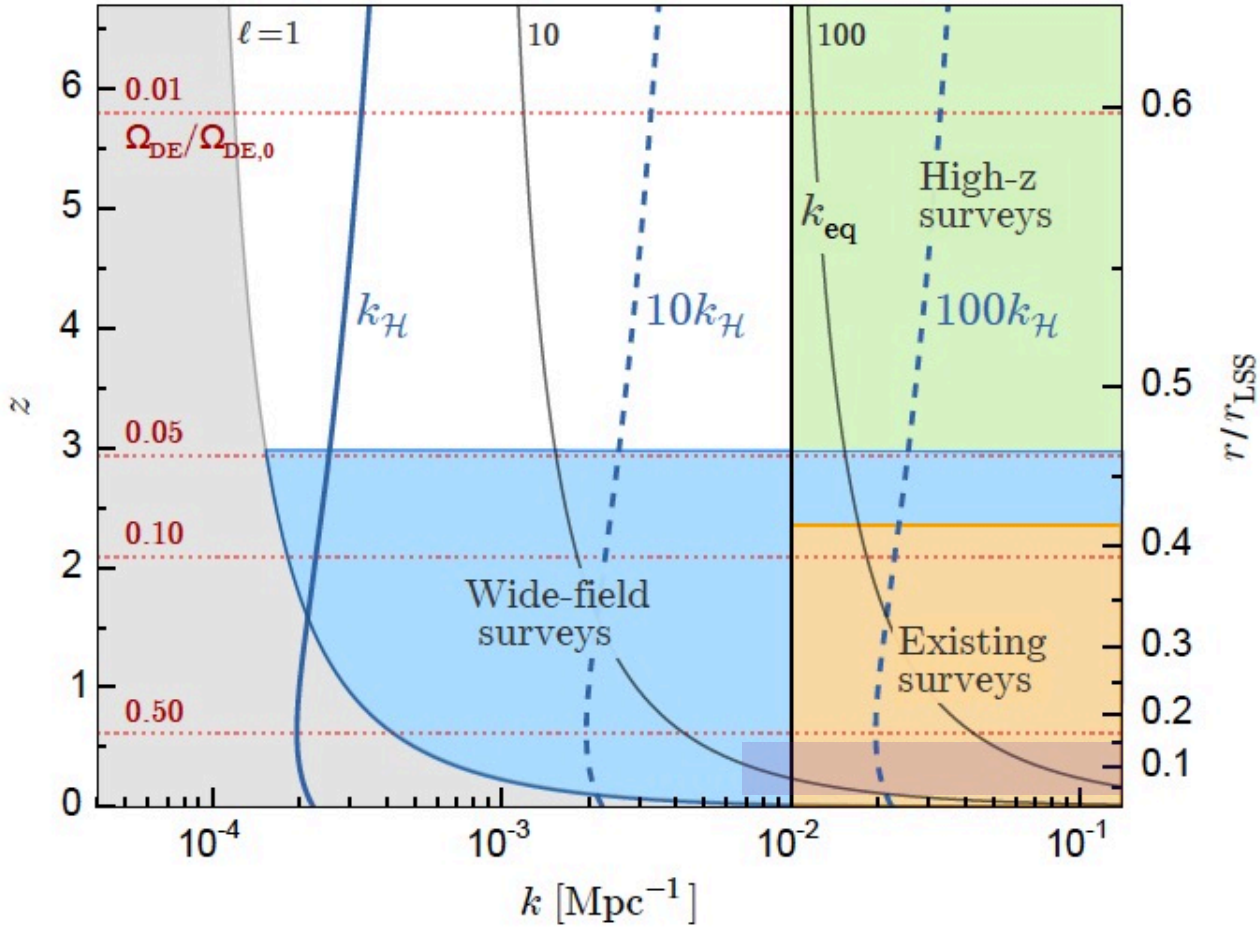
$$k_\parallel^{\max} \sim k_{\rm NL} = 1/\sigma_{\rm NL}$$

$$k_\perp^{\min} \sim k_{\rm area} = 2\pi/\sqrt{r^2 S_{\rm area}} \quad \text{(single dish)}$$

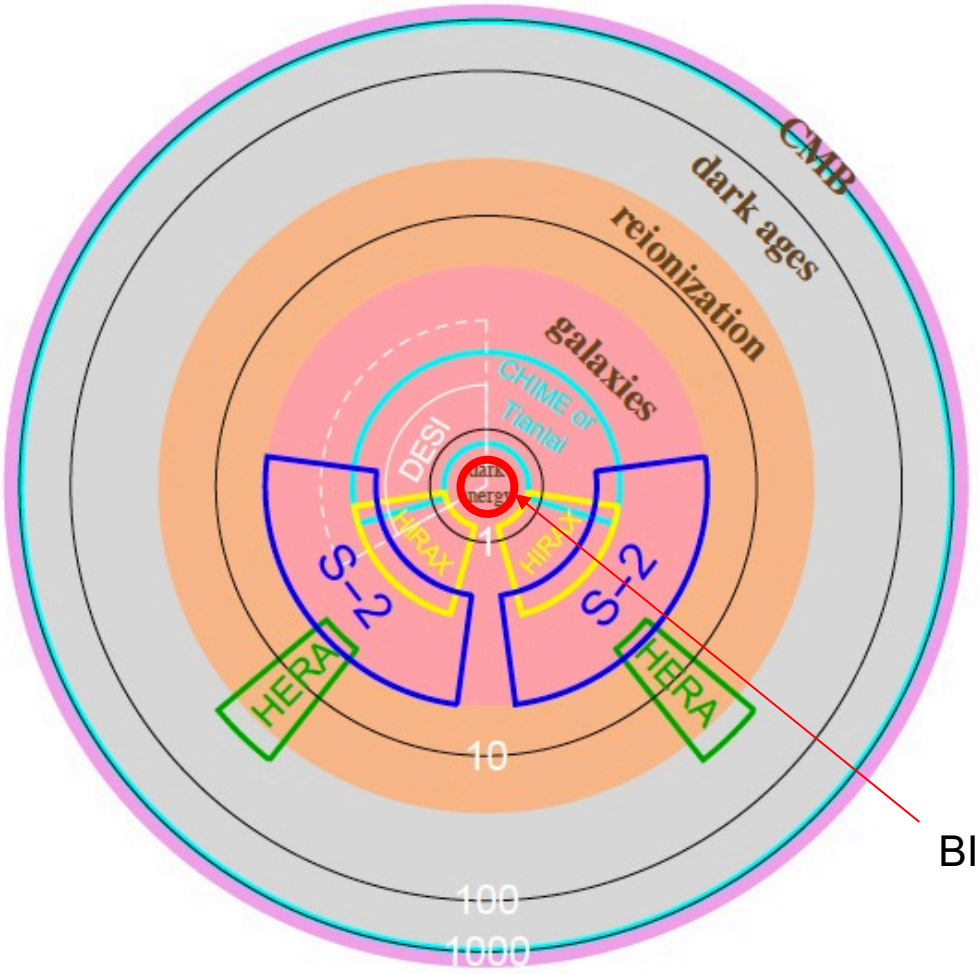
$$\sim k_{D_{\rm min}} = 2\pi D_{\rm min}/r\lambda \quad \text{(interferom.)}$$

$$k_\perp^{\max} \sim k_{\rm FOV} = 2\pi D_{\rm dish}/r\lambda \quad \text{(single dish)}$$

$$\sim k_{D_{\rm max}} = 2\pi D_{\rm max}/r\lambda \quad \text{(interferom.)}.$$



Kovetz et al, (arXiv:1709.09066)

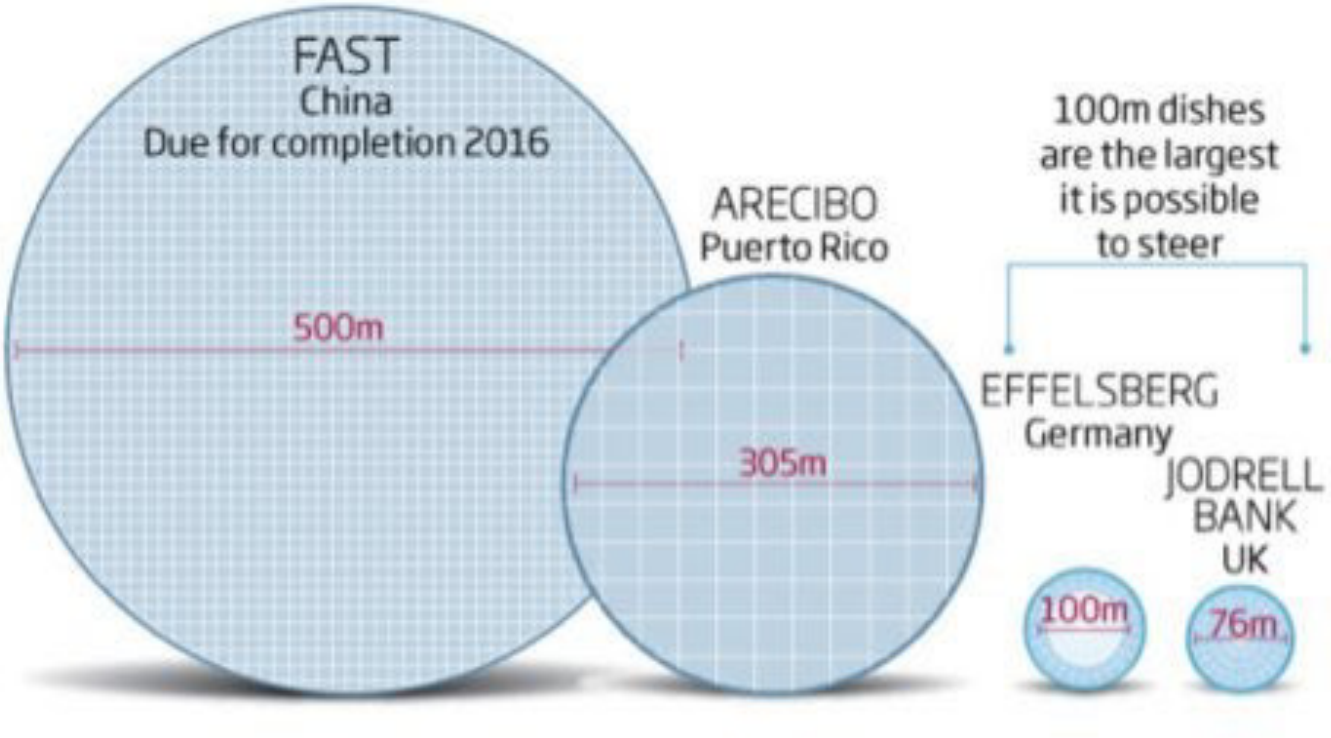


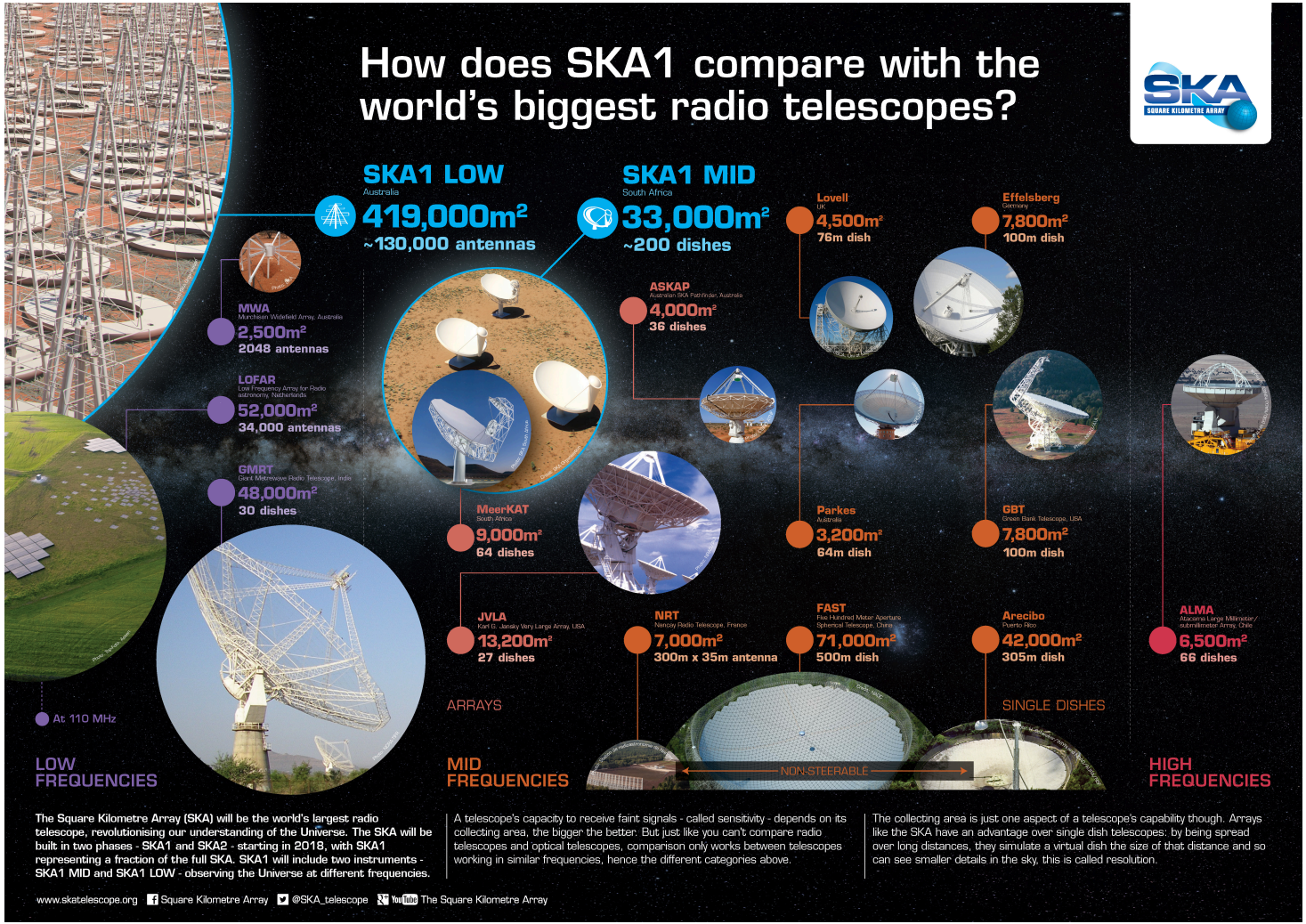
BINGO outer boundary

Ansari et al. (arXiv:1810.09572)

C. A. Wuensche (2021)

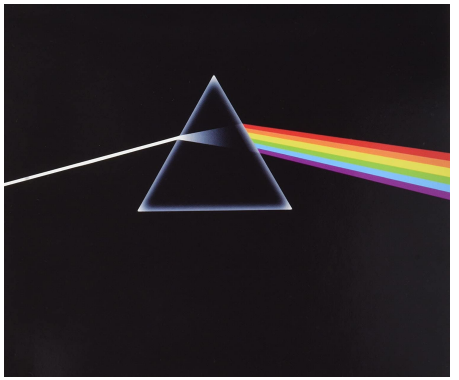
Radio astronomy will get a big boost with FAST, the world's most sensitive radio telescope




How does SKA1 compare with the world's biggest radio telescopes?
SKA
SQUARE KILOMETRE ARRAY
SKA1 LOW
Australia
419,000m²
~130,000 antennas
SKA1 MID
South Africa
33,000m²
~200 dishes
MWA
Murchison Widefield Array, Australia
2,500m²
2048 antennas
LOFAR
Low Frequency Array for Radio astronomy, Netherlands
52,000m²
34,000 antennas
GMRT
Giant Metrewave Radio Telescope, India
48,000m²
30 dishes
At 110 MHz
LOW FREQUENCIES
ASKAP
Australian SKA Pathfinder, Australia
4,000m²
36 dishes
MeerKAT
South Africa
9,000m²
64 dishes
JVLA
Karl G. Jansky Very Large Array, USA
13,200m²
27 dishes
ARRAYS
Lovell
UK
4,500m²
76m dish
Effelsberg
Germany
7,800m²
100m dish
Parkes
Australia
3,200m²
64m dish
GBT
Green Bank Telescope, USA
7,800m²
100m dish
NRT
Nancay Radio Telescope, France
7,000m²
300m x 35m antenna
FAST
Five Hundred Meter Aperture Spherical Telescope, China
71,000m²
500m dish
Arecibo
Puerto Rico
42,000m²
305m dish
ALMA
Atacama Large Millimeter/submillimeter Array, Chile
6,500m²
66 dishes
SINGLE DISHES
NON-STEERABLE
MID FREQUENCIES
HIGH FREQUENCIES
The Square Kilometre Array (SKA) will be the world's largest radio telescope, revolutionising our understanding of the Universe. The SKA will be built in two phases - SKA1 and SKA2 - starting in 2018, with SKA1 representing a fraction of the full SKA. SKA1 will include two instruments - SKA1 MID and SKA1 LOW - observing the Universe at different frequencies.
A telescope's capacity to receive faint signals - called sensitivity - depends on its collecting area, the bigger the better. But just like you can't compare radio telescopes and optical telescopes, comparison only works between telescopes working in similar frequencies, hence the different categories above.
The collecting area is just one aspect of a telescope's capability though. Arrays like the SKA have an advantage over single dish telescopes: by being spread over long distances, they simulate a virtual dish the size of that distance and so can see smaller details in the sky, this is called resolution.
www.skatelescope.org
Square Kilometre Array
@SKA_telescope
The Square Kilometre Array

A (non-exhaustive) list of current 21cm instruments

- The instruments listed aere either operating, under construction or planned
- They are, broadly, "single-dish" or interferometers
- The frequency range covered goes from ~ MHz to ~ GHz
- There are arrays, transit telescopes and "strange" antennas
- Operating all over the terrestrial globe
- Nothing still operating (but being thought of...) in the Dark Side of the Moon!!!



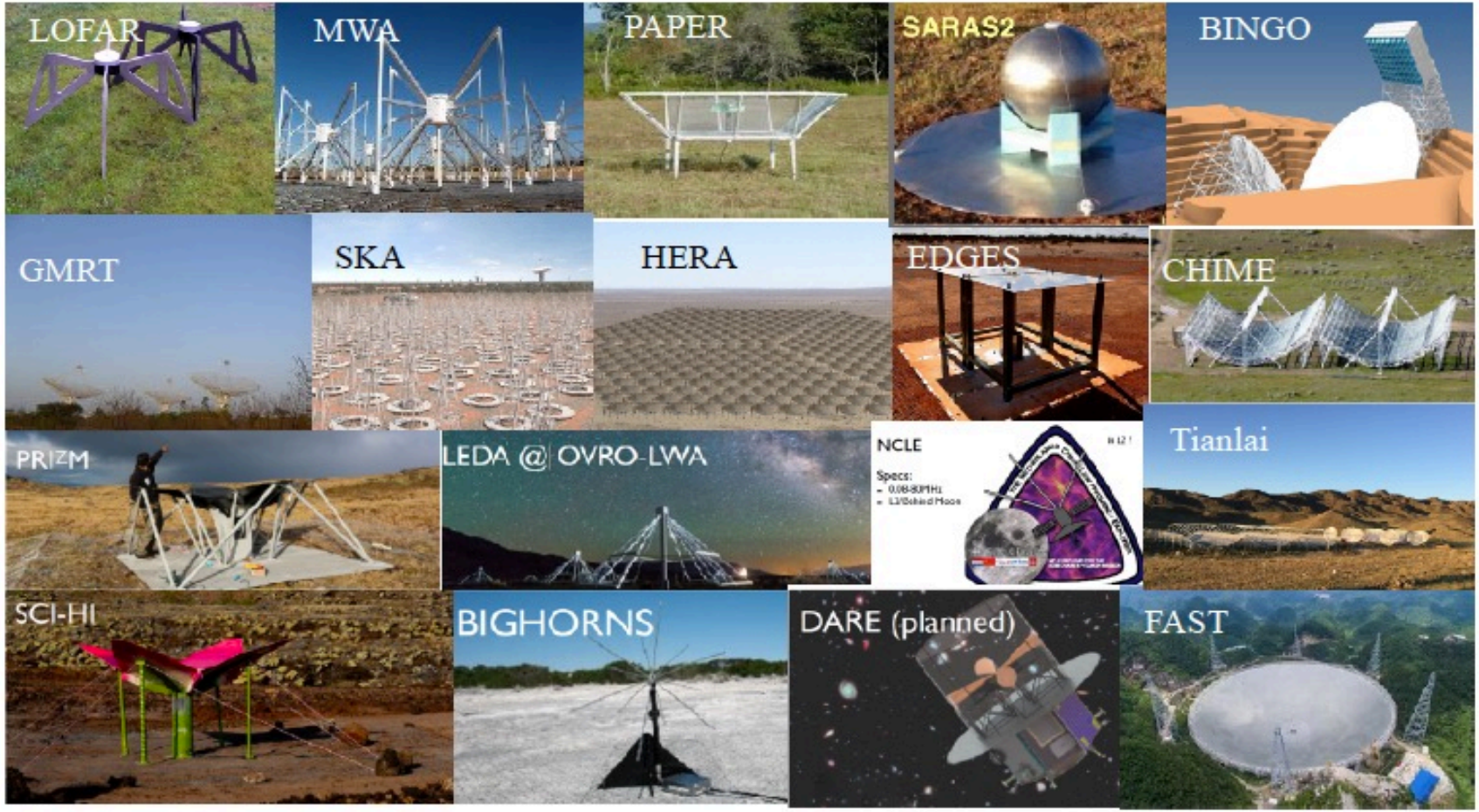
Experiment	Line	Frequency	Redshift range	Location
HERA	HI	50 – 250 MHz	5 – 27	South Africa
SKA-LOW	HI	50 – 350 MHz	3 – 7	Australia
CCAT-prime	[CII]	185 – 440 GHz	3.3 – 9.3	Chile
TIME	[CII]	200 – 300 GHz	5.3 – 8.5	North America
CONCERTO	[CII]	200 – 360 GHz	4.3 – 8.5	Chile
COPSS	CO	27 – 35 GHz	2.3 – 3.3	North America
mmIME	CO, [CII]	300, 100, 30 GHz	1 – 5	various
AIM-CO	CO	86 – 102 GHz	1.2 – 1.7, 2.4 – 3.0	China
COMAP	CO	26 – 34 GHz	2.4 – 3.4, 5.8 – 7.8	North America
STARFIRE	[CII], NII	714 – 1250 GHz	0.5 – 1.5	Sub-orbit (balloon)
SPHEREx	Hα (Hβ, [OII], [OIII]), Lyα	60 – 400 THz	0.1 – 5, 5.2 – 8	Space
CHIME	HI	400 – 800 MHz	0.8 – 2.5	North America
HIRAX	HI	400 – 800 MHz	0.8 – 2.5	South Africa
SKA-MID	HI	350 MHz – 14 GHz	0 – 3	South Africa
BINGO	HI	939 – 1238 MHz	0.13 – 0.48	South America

Kovetz et al, (arXiv:1709.09066, 2017)

Table 4-1. *Parameters for various intensity mapping instruments described below.*

Experiment	Frequency Range	Antenna	Presence of Balun	Calibration Scheme	Type of Spectrometer
SARAS 2	40 – 200 MHz	Spherical Monopole antenna	No	Noise source coupled into system via power combiner without Dicke switch	Cross-correlation
EDGES	100 – 200 MHz (High-Band) 50 – 100 MHz (Low-Band)	Blade Antenna	Yes	Switching between antenna and noise source	Auto-correlation
BIGHORNS	70 – 200 MHz	Conical log-spiral antenna	Yes	Switching between antenna and reference load	Auto-correlation
SCI-HI	40 – 130 MHz	HIbiscus antenna	Yes	Switching between antenna, 50 Ω, 100 Ω and short termination	Auto-correlation
LEDA	40 – 85 MHz	Dual-polarized dipole antenna	Yes	Switching between antenna and noise source combined with cross-correlation from other antennas for antenna gain and beam estimation	Auto-correlation

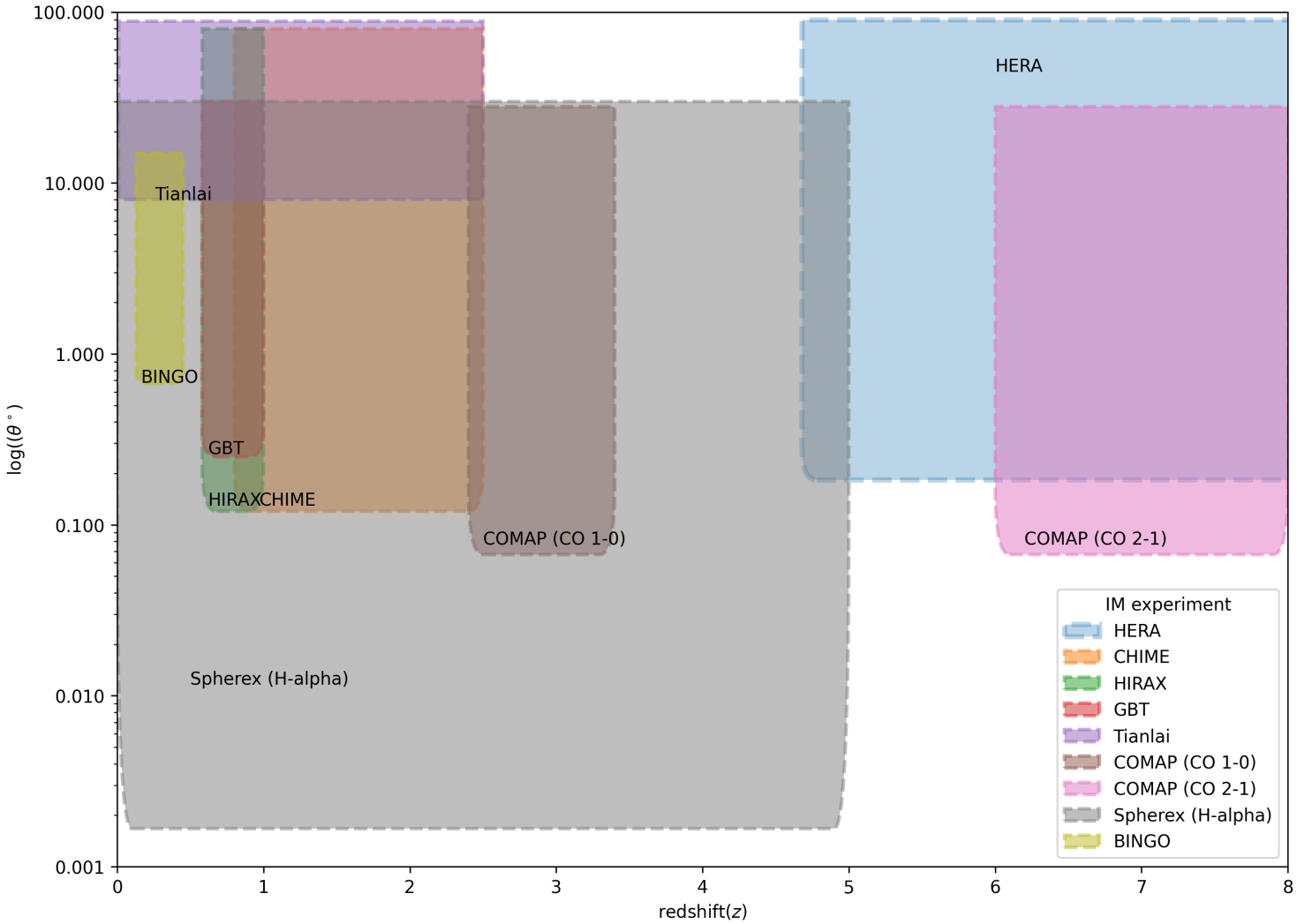
Singh et al. (arxiv:1710.01101, 2017)


LOFAR
MWA
PAPER
SARAS2
BINGO
GMRT
SKA
HERA
EDGES
CHIME
PRIZM
LEDA @ OVRO-LWA
NCLE
Specs:
Tianlai
SCI-HI
BIGHORNS
DARE (planned)
FAST

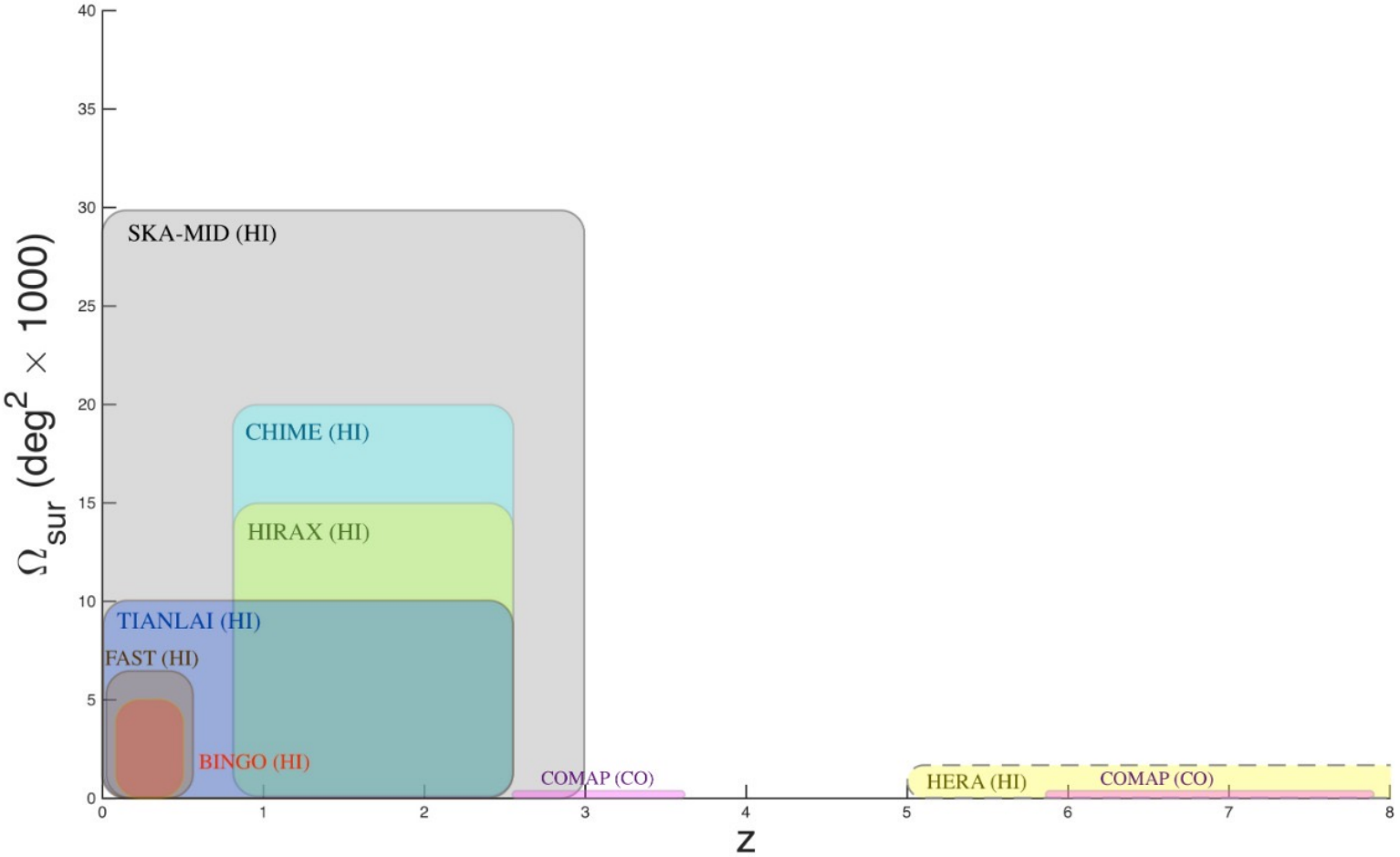
Intensity Mapping experiments status

Probe		Results Published	Currently Observing / Under Construction		Planned
HI	Low z	GBT Parkes	CHIME HIRAX →	SKA BINGO	
	Med. z		PRIZM TAINLAI →	GBT-HIM	
		PAPER	HERA →		
Lyalpha Hbeta Halpha					SPHEREX
CO		COPSS	mmIME	AIM-CO COMAP	
[CII]				TIME CONCERTO	CCAT-p PIXIE
[NII]				STARFIRE	
[OI]					

credit: Abigail Crites



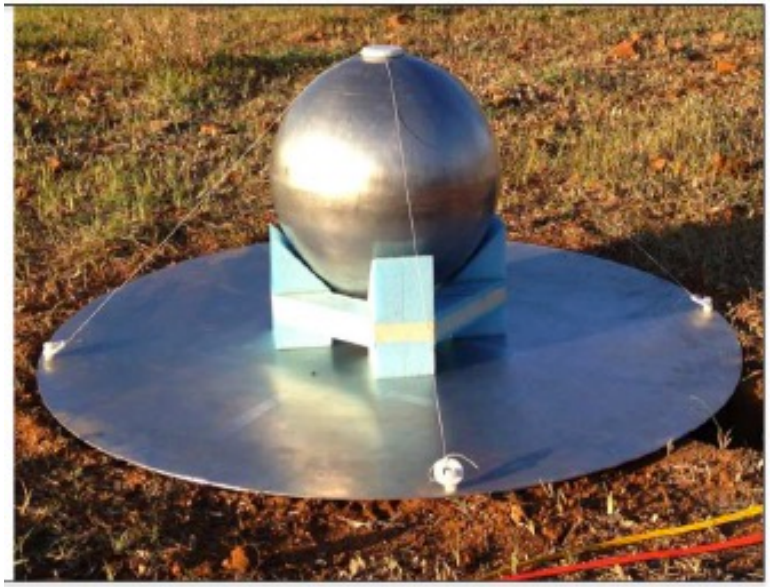
Abdalla et al. (arXiv:2107.01633, 2021



Abdalla et al. (arXiv:2107.01633, 2021

SARAS 2 (Shaped Antenna measurement of the background RAdio Spectrum)

- Class: single dish
- Operating mode: spectral radiometry
- Frequency interval: 40 – 200 MHz
- Angular resolution: full sky sensitivity
- Other relevant info: designed to detected the sky-averaged 21cm signal

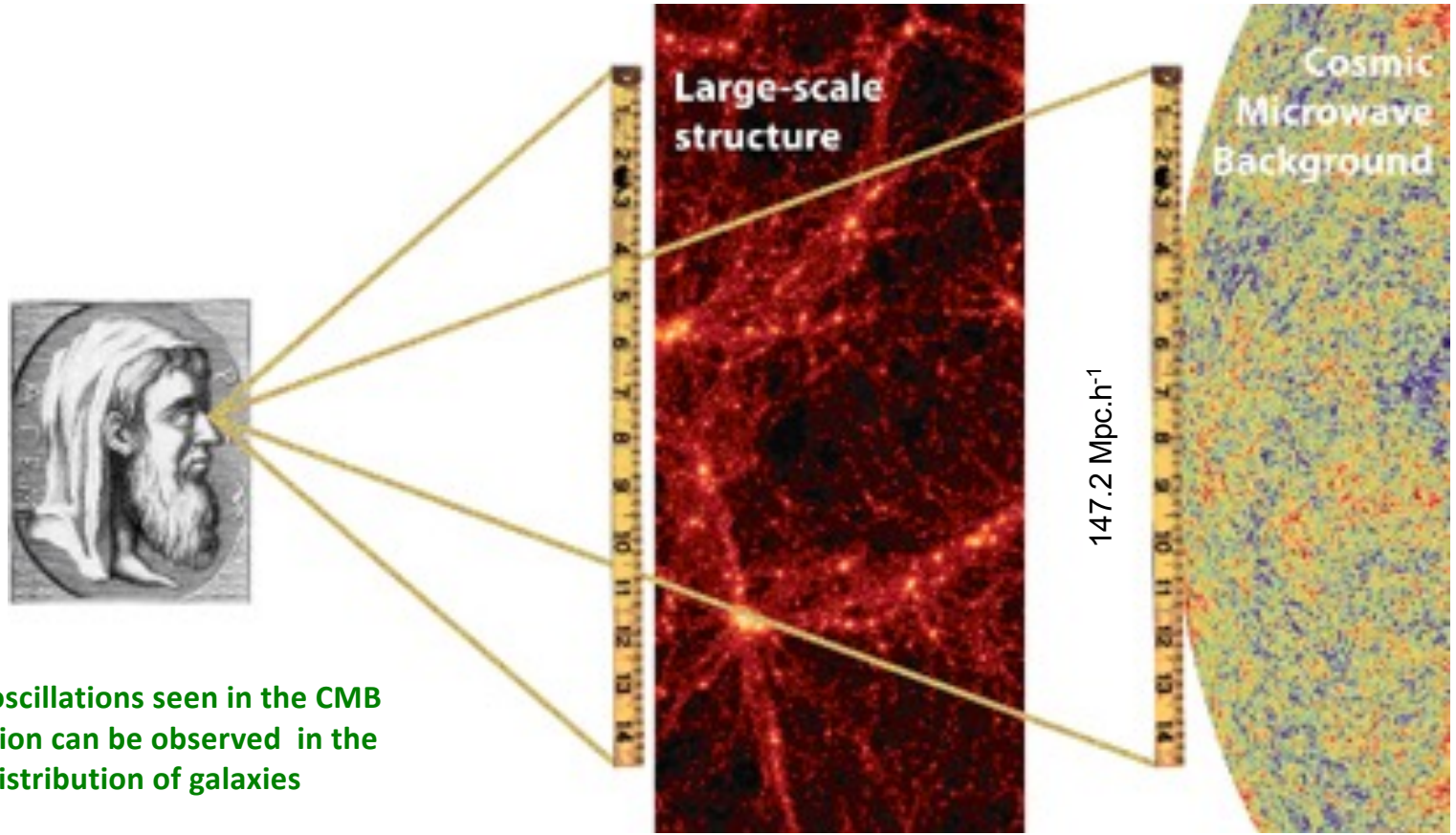


Singh et al. (arxiv:1711.11281, 2017)

BARYON ACOUSTIC OSCILLATIONS (BAO)

21 cm cosmology and BAO

Source: ESA



Baryon oscillations seen in the CMB distribution can be observed in the spatial distribution of galaxies

C. A. Wuensche (2021)

BAO highlights

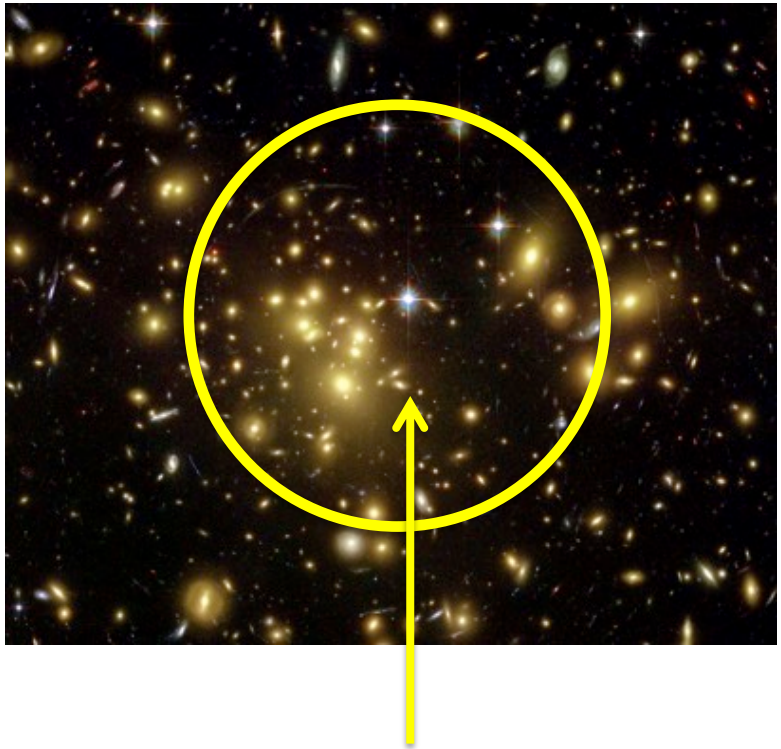
- Acoustic waves imprinted on CMB 380,000 years after Big Bang
- Acoustic scale **D** set by distance light travelled at that time
  - Known precisely from CMB power spectrum
  - **D=147.18±0.29 Mpc (Planck Collaboration 2018 - VI)**
- Universe is reasonably well understood from t ~ 10^{-6}s to t ~ 380.000 years and then after Cosmic Dawn (t ~ 180 Myears)
- History of matter evolution can be traced via HI (and its "disappearance") from z=20 to z=0

Alternative to optical BAO: HI Intensity mapping

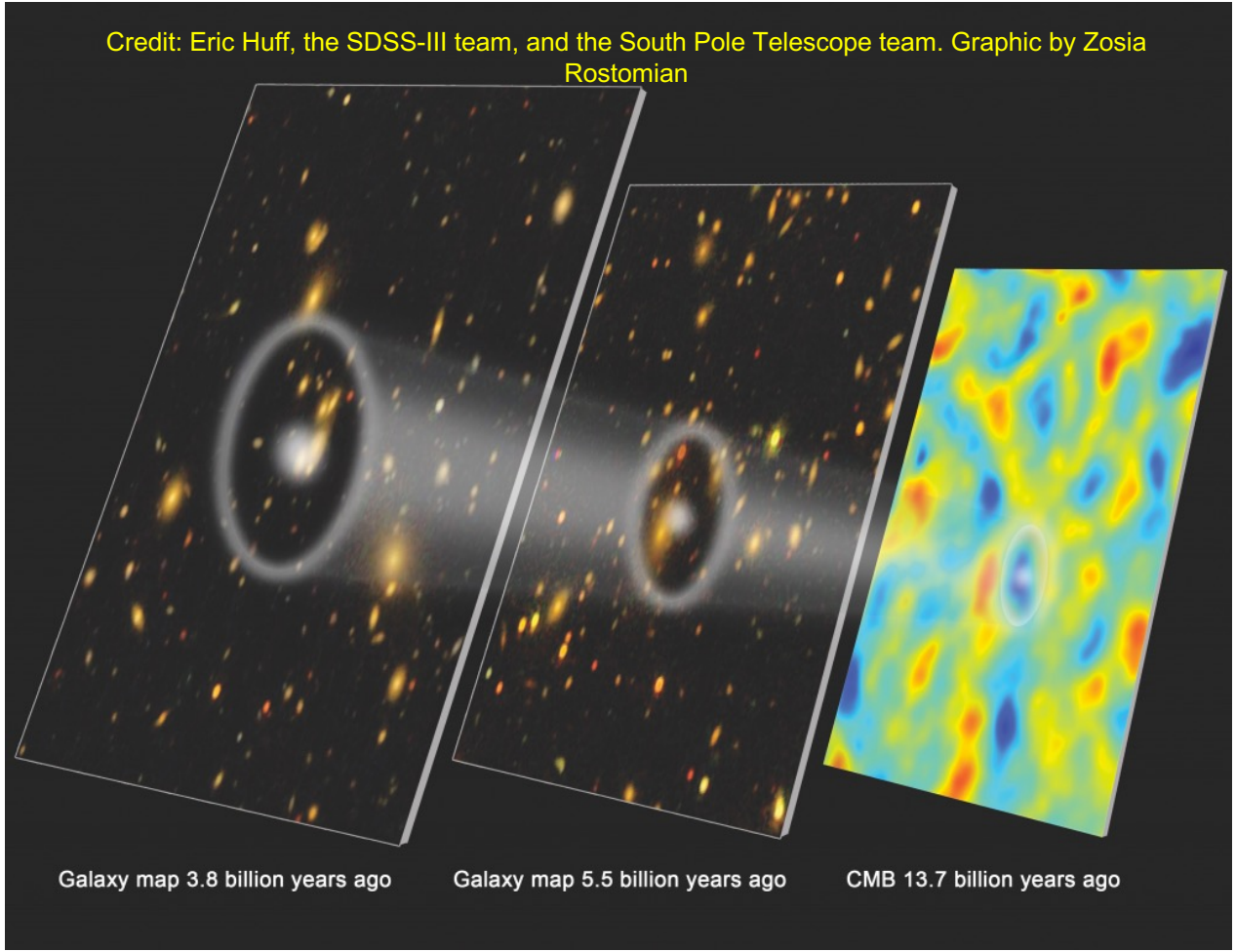
- Use relatively large beam on the sky
  - Measure HI *fluctuations*
- HI intensity mapping can be used as mass tracer, probing distortions in redshift space
- No competition in the radio
- Complementary to large optical surveys
- Similar to CMB, using:

$$\Delta T_{CMB} = \Delta T_{CMB}(\theta, \phi, z = 1100)$$

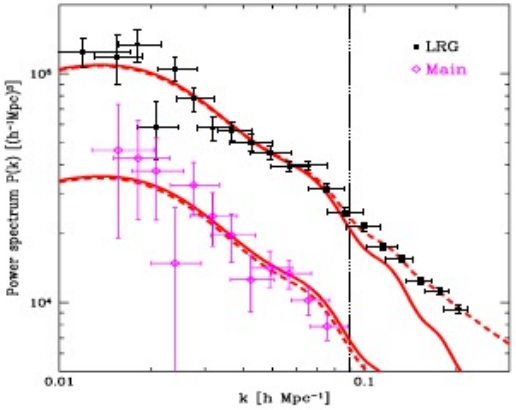
$$\Delta T_{HI} = \Delta T_{HI}(\theta, \phi, z)$$

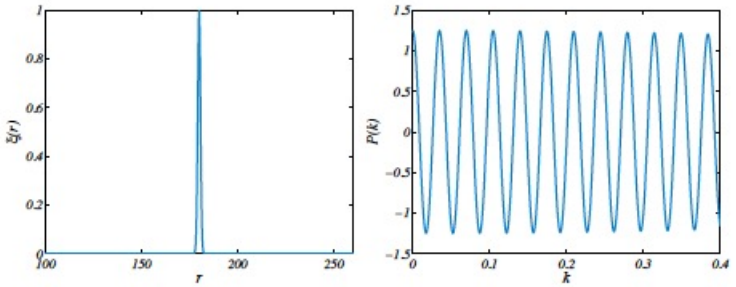


- Large beam on the sky (≈1 deg) contains many galaxies.
- HI signal is measured through its overall intensity

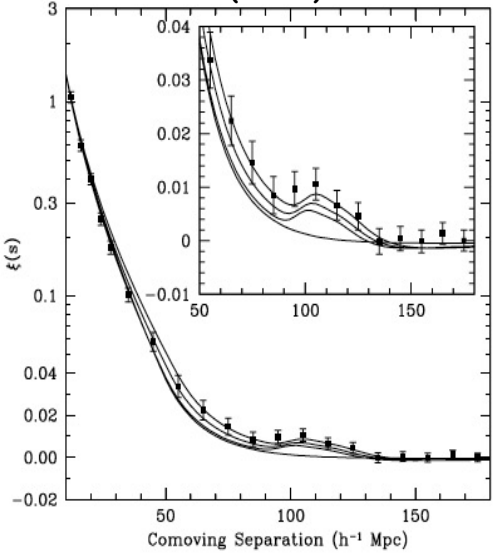

Credit: Eric Huff, the SDSS-III team, and the South Pole Telescope team. Graphic by Zosia Rostomian
Galaxy map 3.8 billion years ago
Galaxy map 5.5 billion years ago
CMB 13.7 billion years ago

Tegmark et al. (2006).



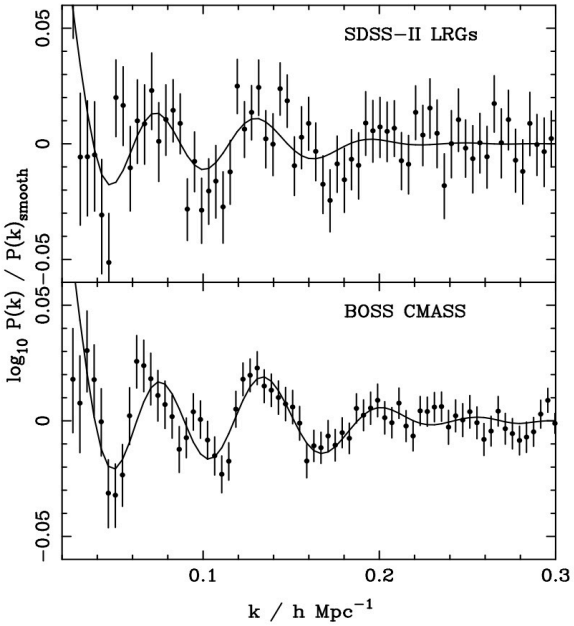


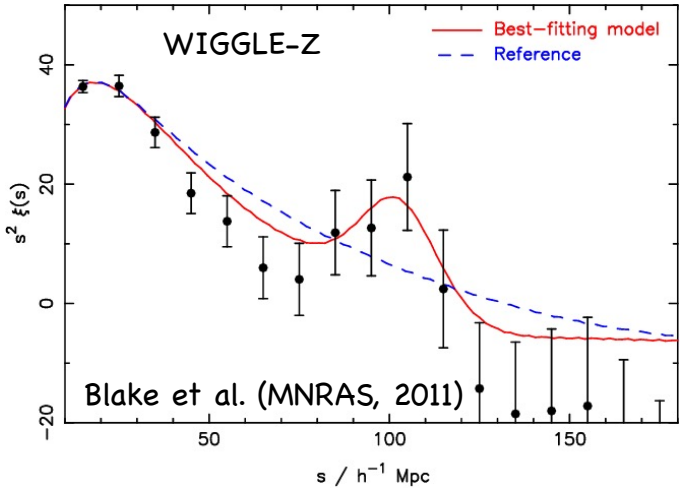
Eisenstein et al. (2005)



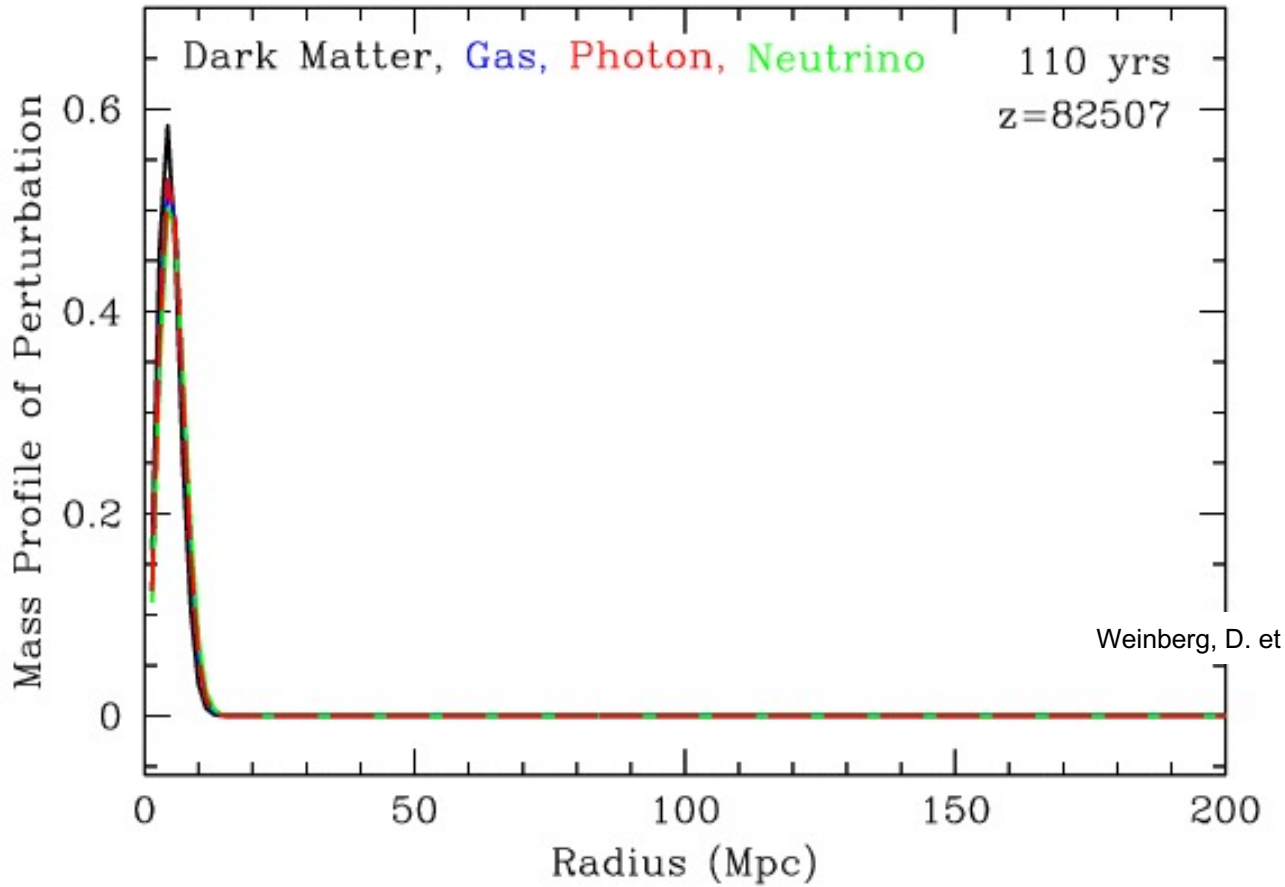
P(k) and $\xi(r)$ are Fourier pairs!!!! A peak in the correlation function (r) space corresponds to oscillations in the power spectrum (k) space

Anderson et al. (2012).





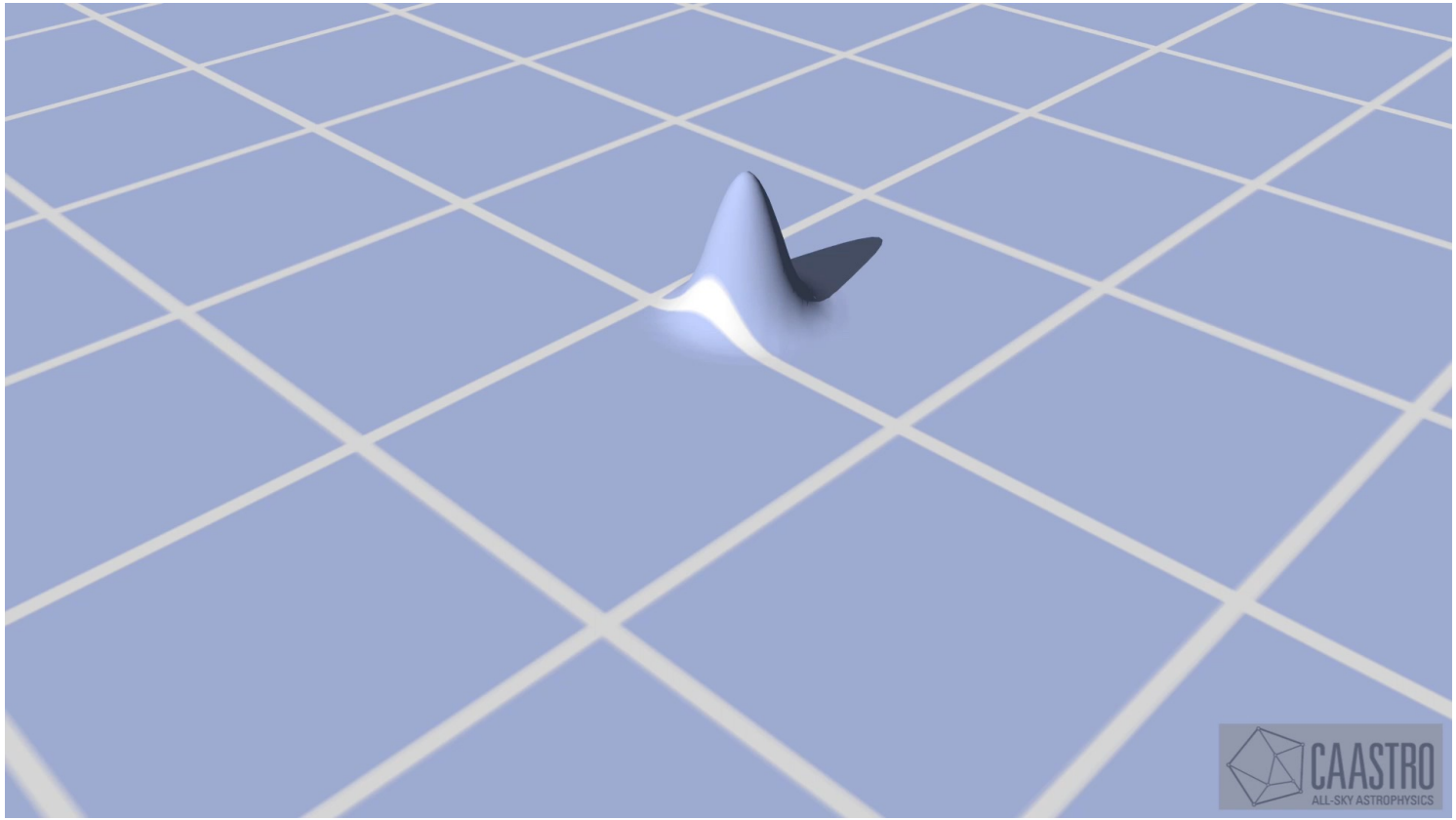
The evolution of perturbations for various cosmic components, in different cosmic times.



Weinberg, D. et al (2013)

After decoupling there is a wave of matter and dark matter, which will gravitationally converge to a common radius.

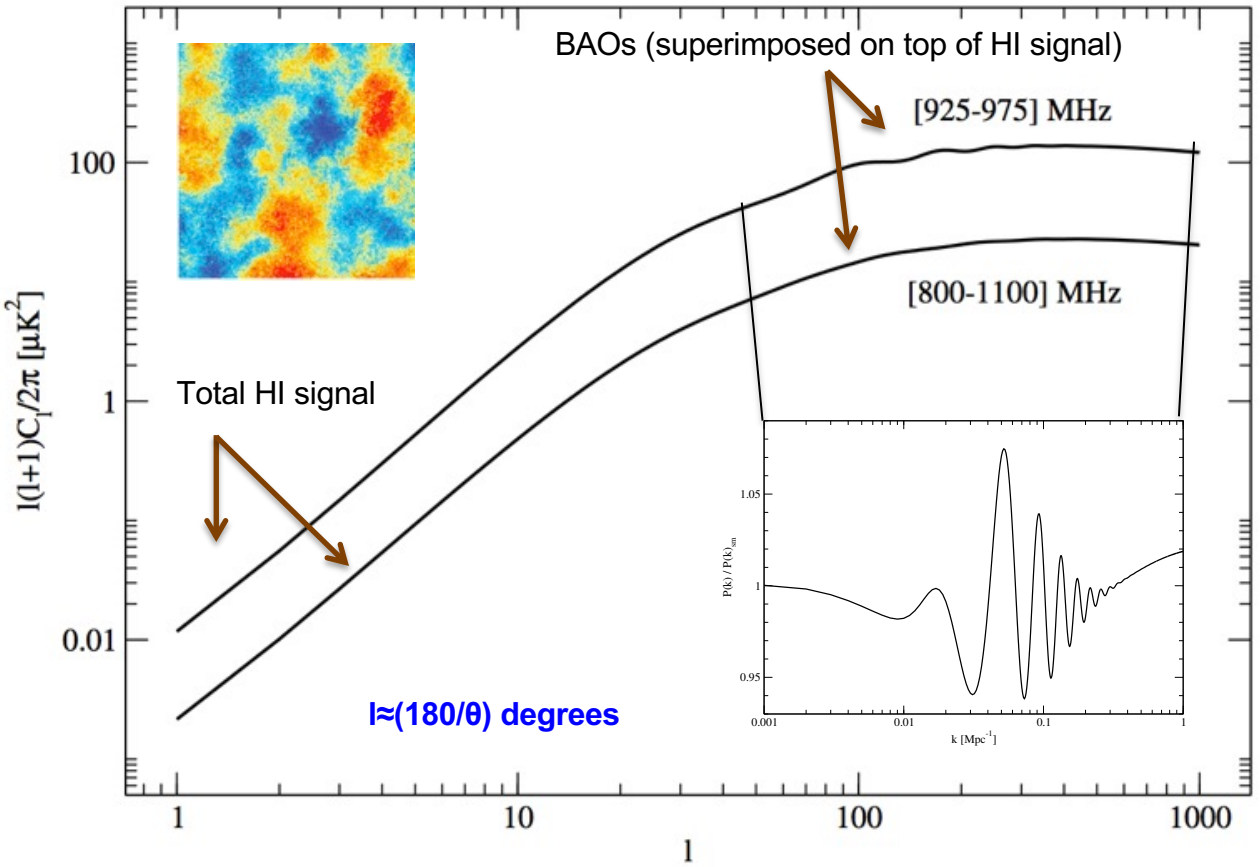
Animation: http://burro.case.edu/Academics/Astr328/Notes/StructForm/BAO.html



Source: CAASTRO (Centre of Excellence for All-sky Astrophysics), https://www.youtube.com/watch?v=jpXuYc-wzk4

The HI signal power spectrum

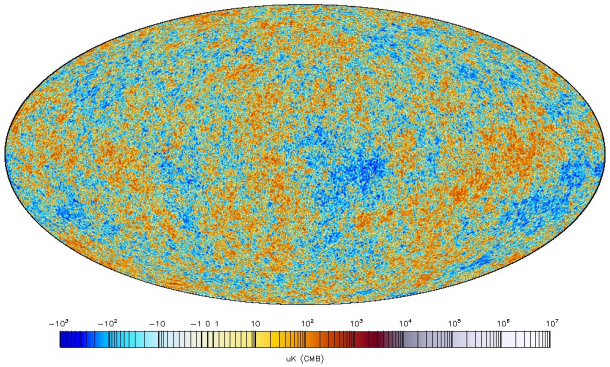
Cosmological HI signal is weak! (≈100 μK rms) and on degree scales $\bar{T}_{\rm obs}(z) = 44\,\mu{\rm K}\left(\frac{\Omega_{\rm H_I}(z)h}{2.45\times10^{-4}}\right)\frac{(1+z)^2}{E(z)}$

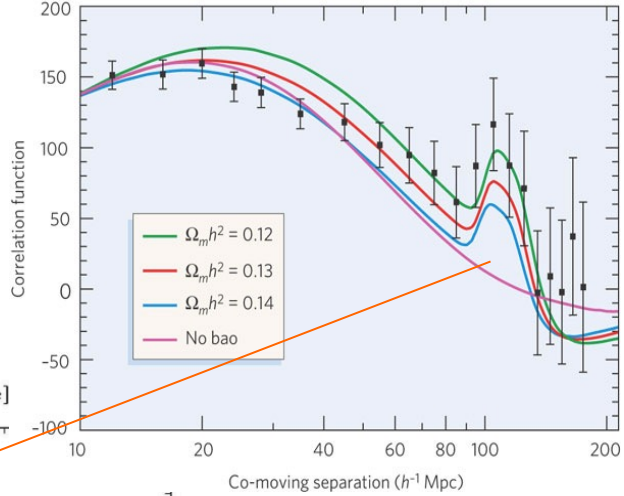


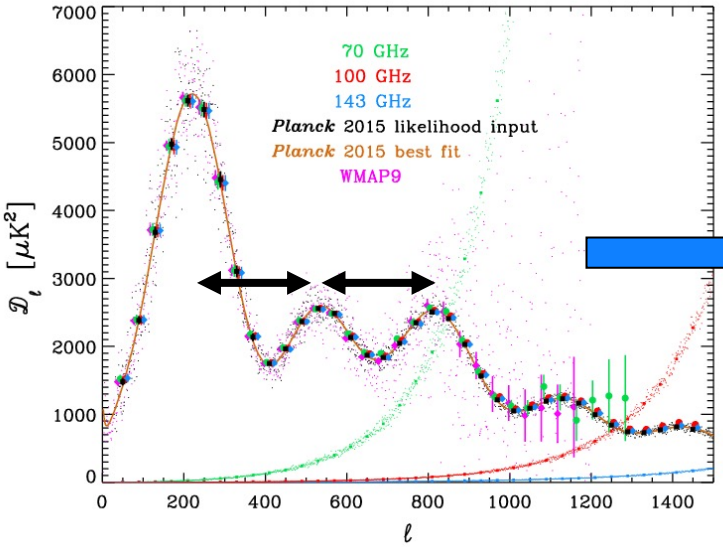
Battye et al. 2013)

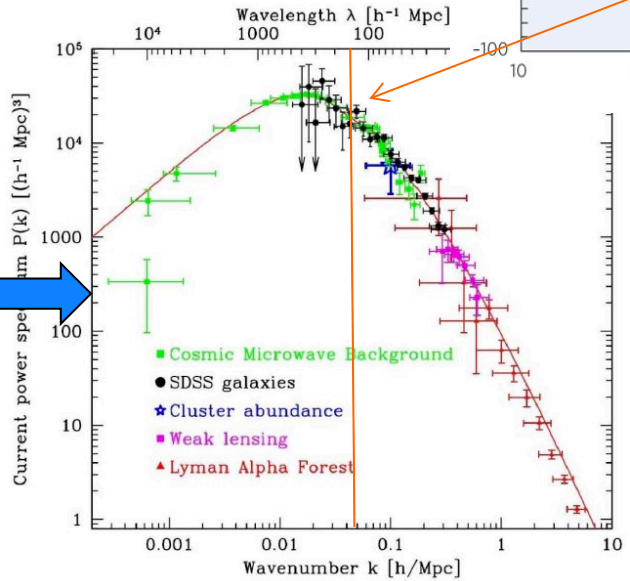
C. A. Wuensche (2021)

Temperature x matter fluctuations



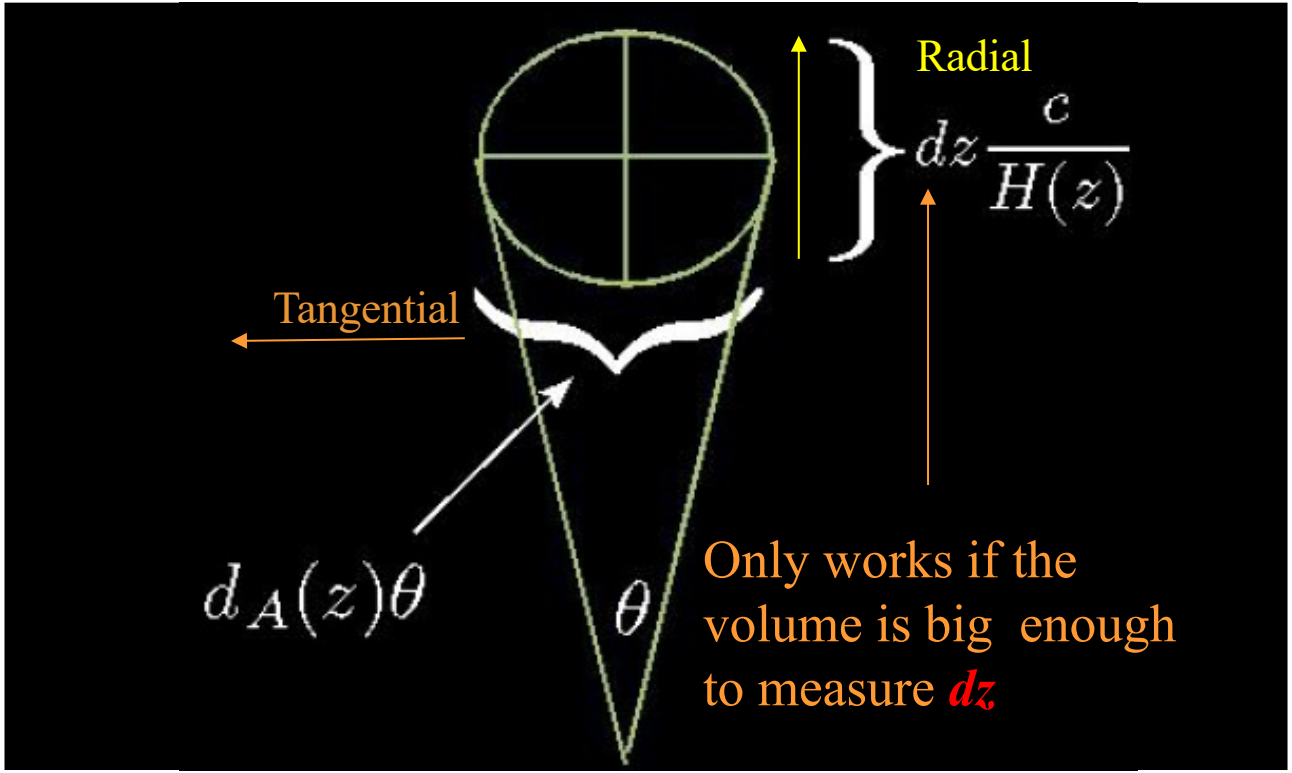






C. A. Wuensche (2021)

The Beauty of Standard Volumes

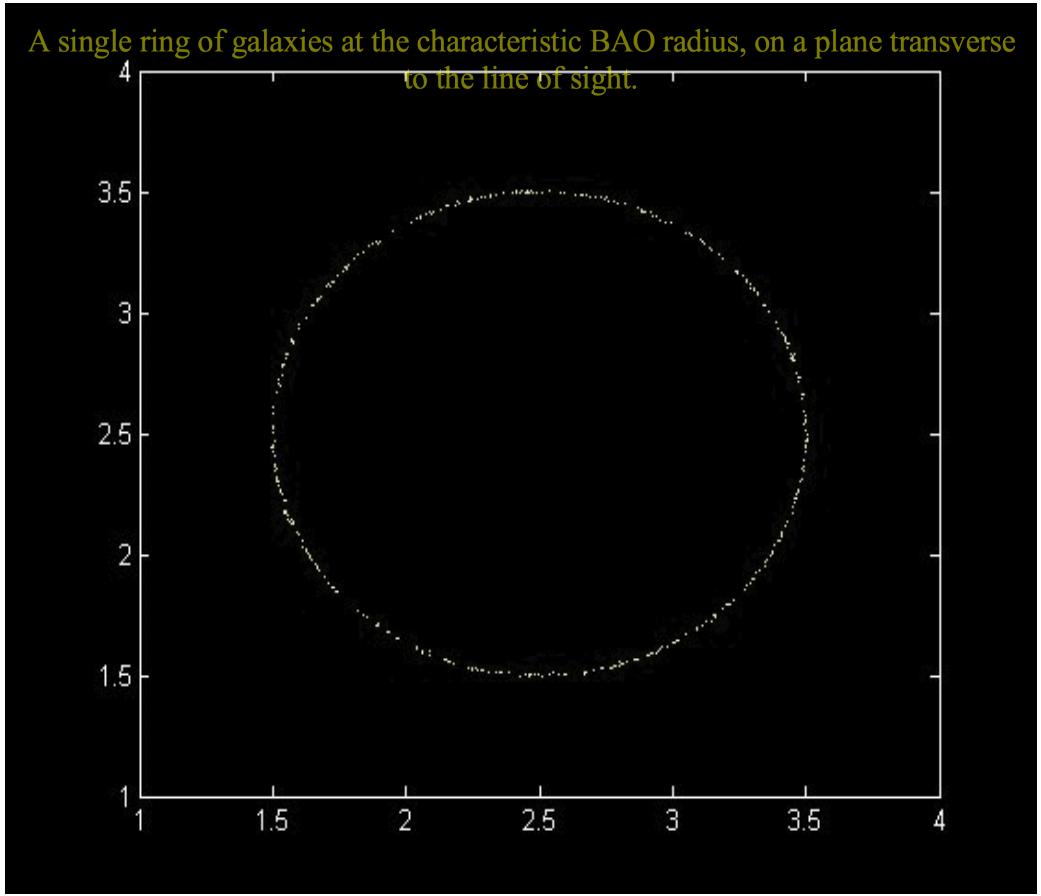


$$H(z) = \frac{c\Delta(z)}{s_{\parallel}(z)}$$

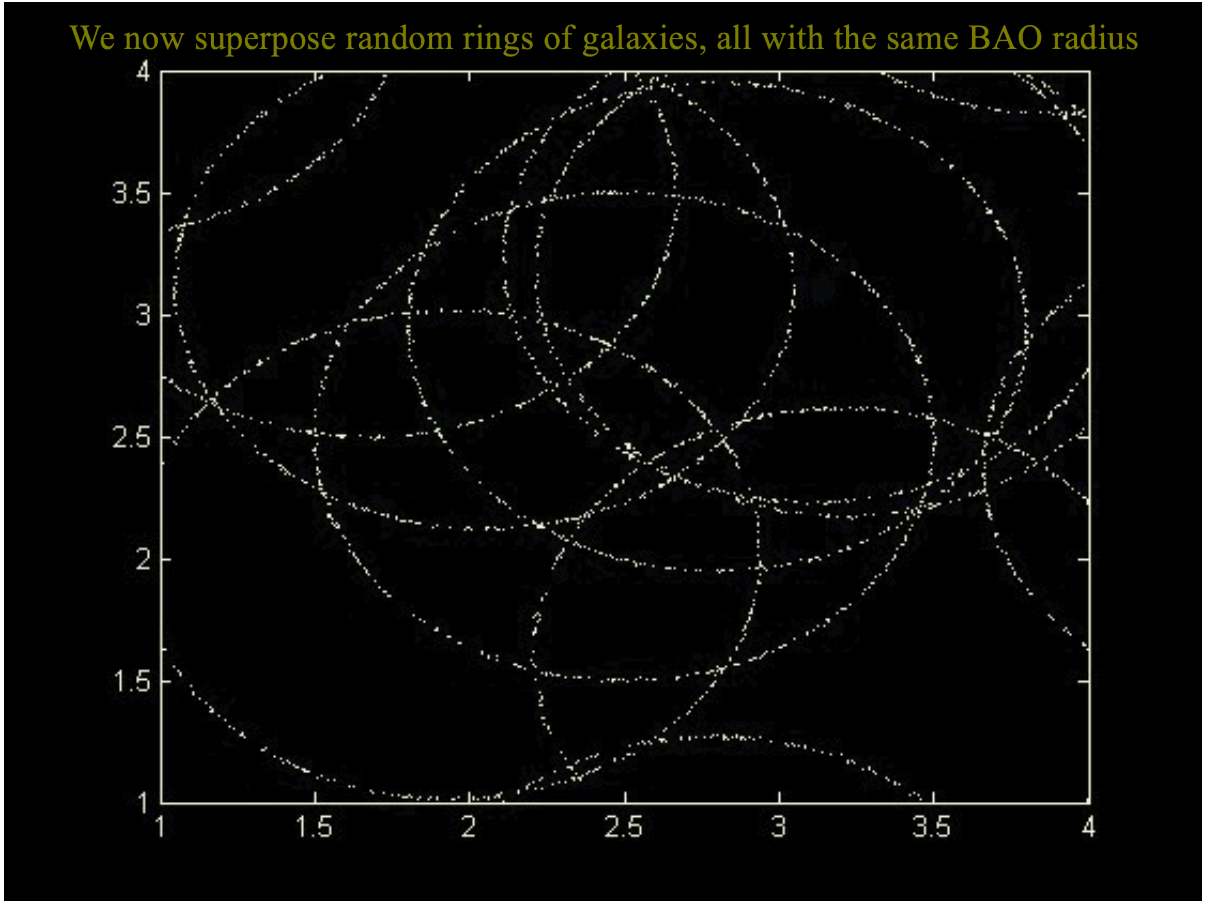
$$d_A(z) = \frac{s_{\perp}(z)}{\Delta\theta(1+z)}$$

Next related slides from Bassett & Hlozek (2009)

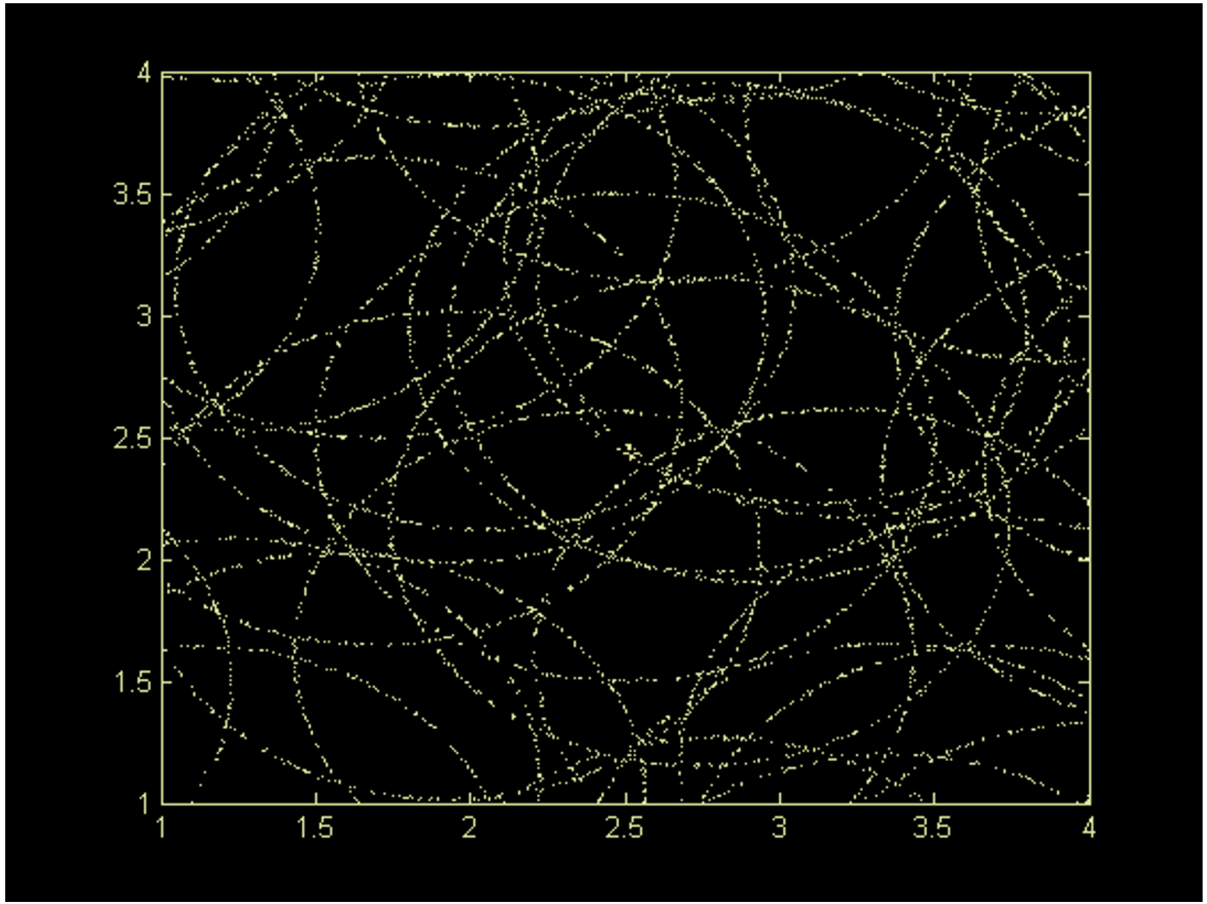
Rings of Power Superposed



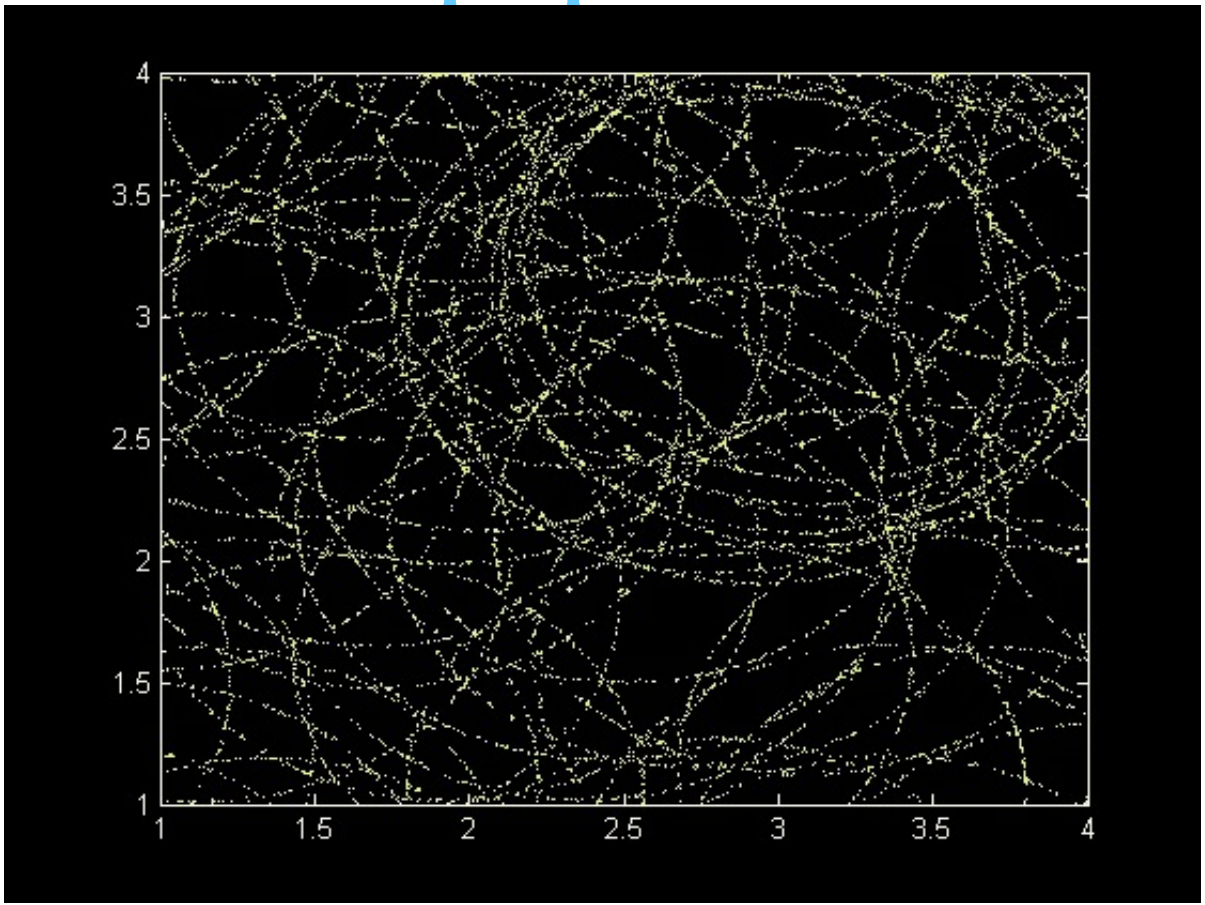
Rings of Power Superposed



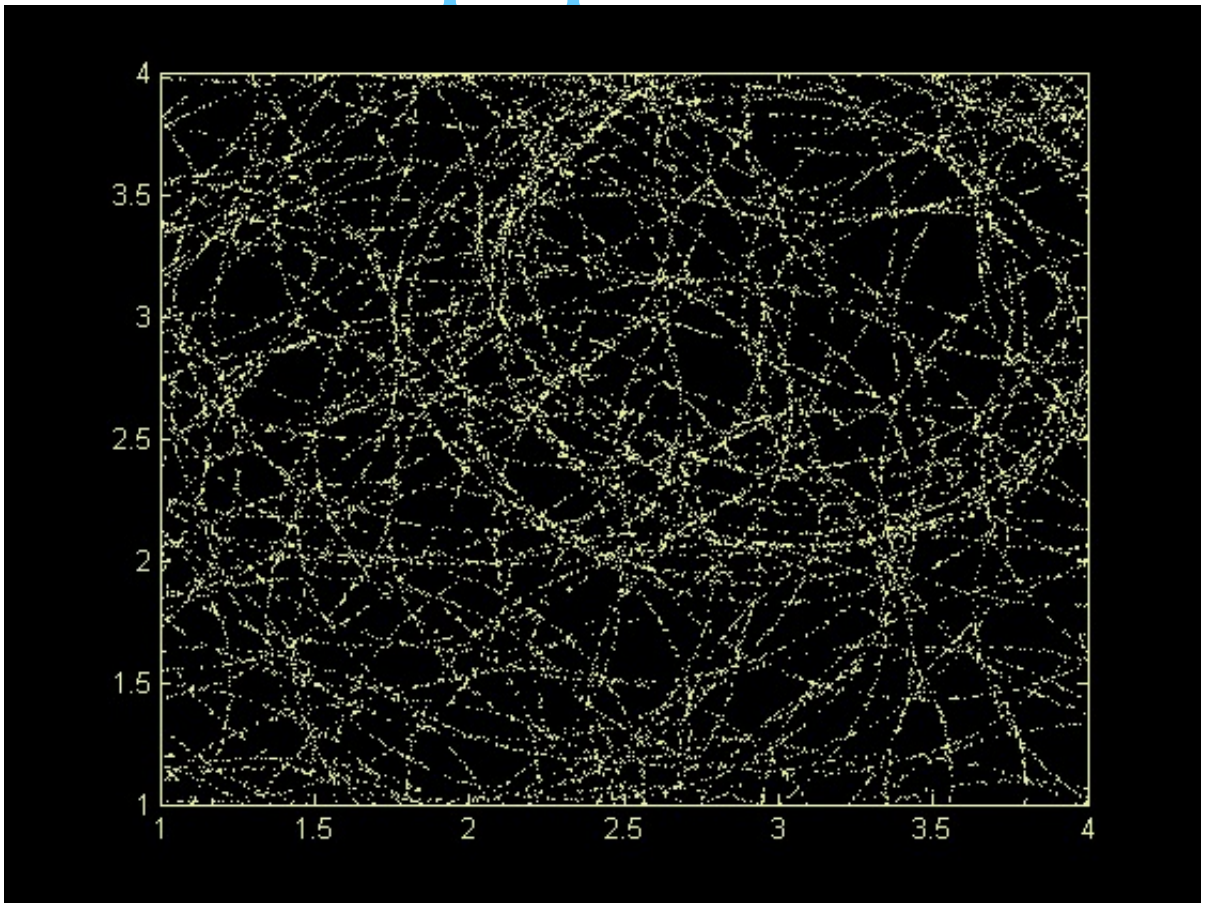
Rings of Power Superposed



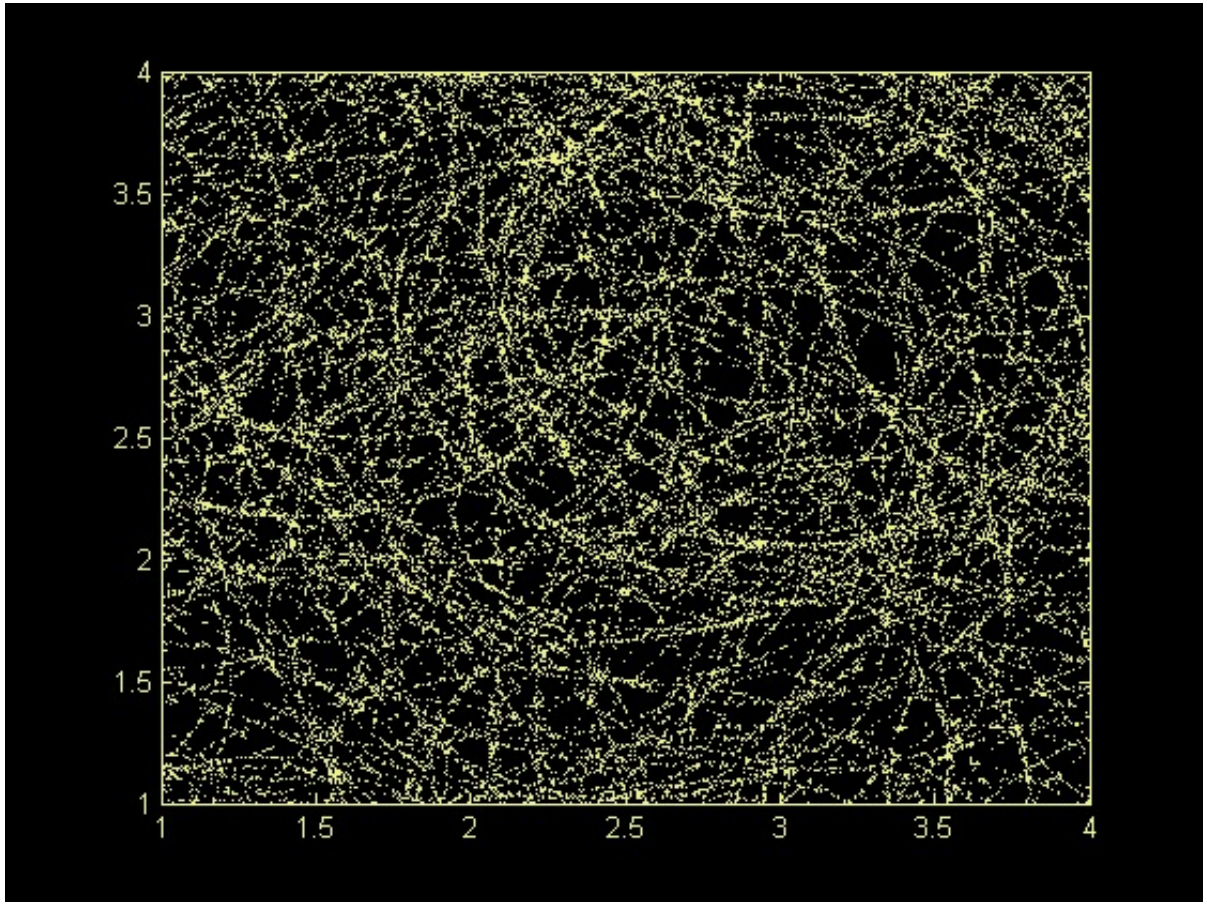
Rings of Power Superposed



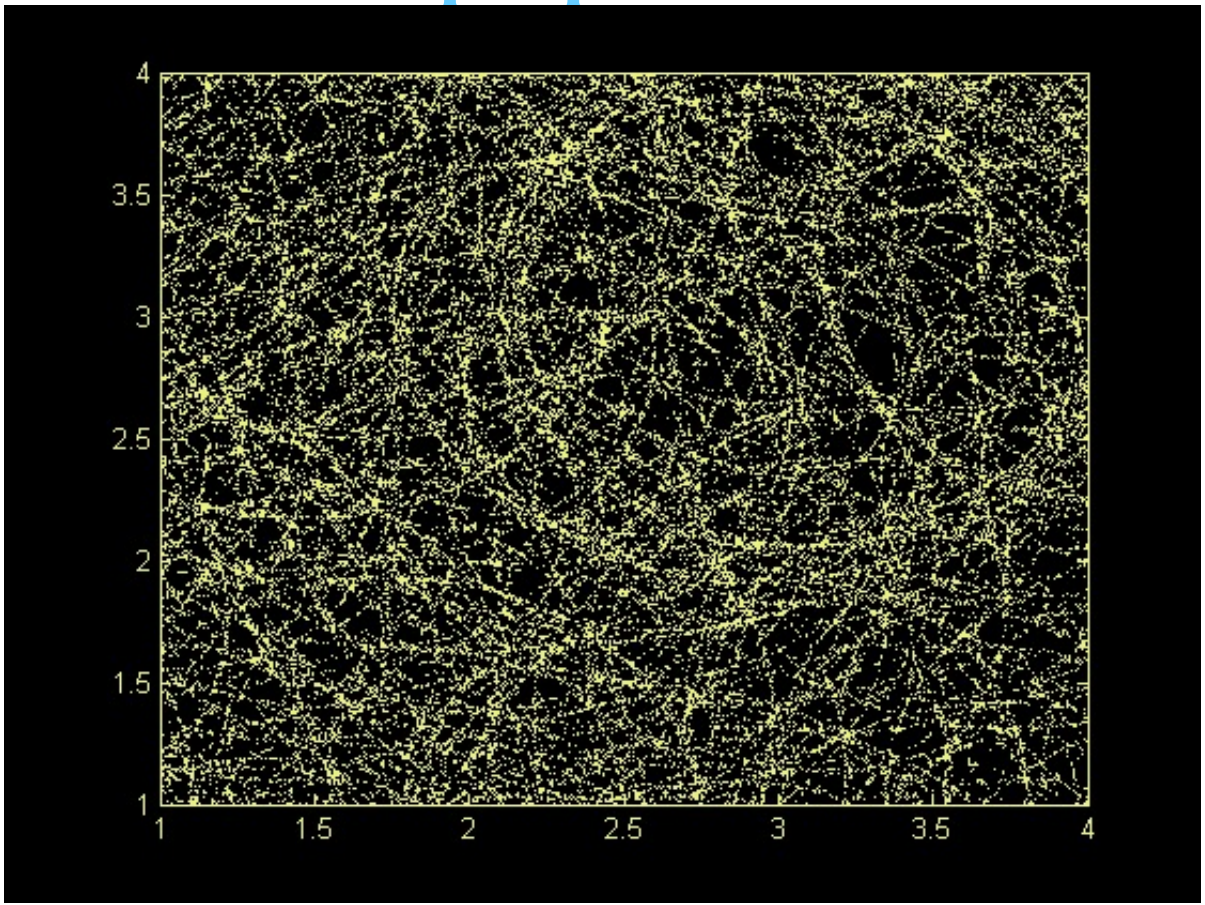
Rings of Power Superposed



Rings of Power Superposed

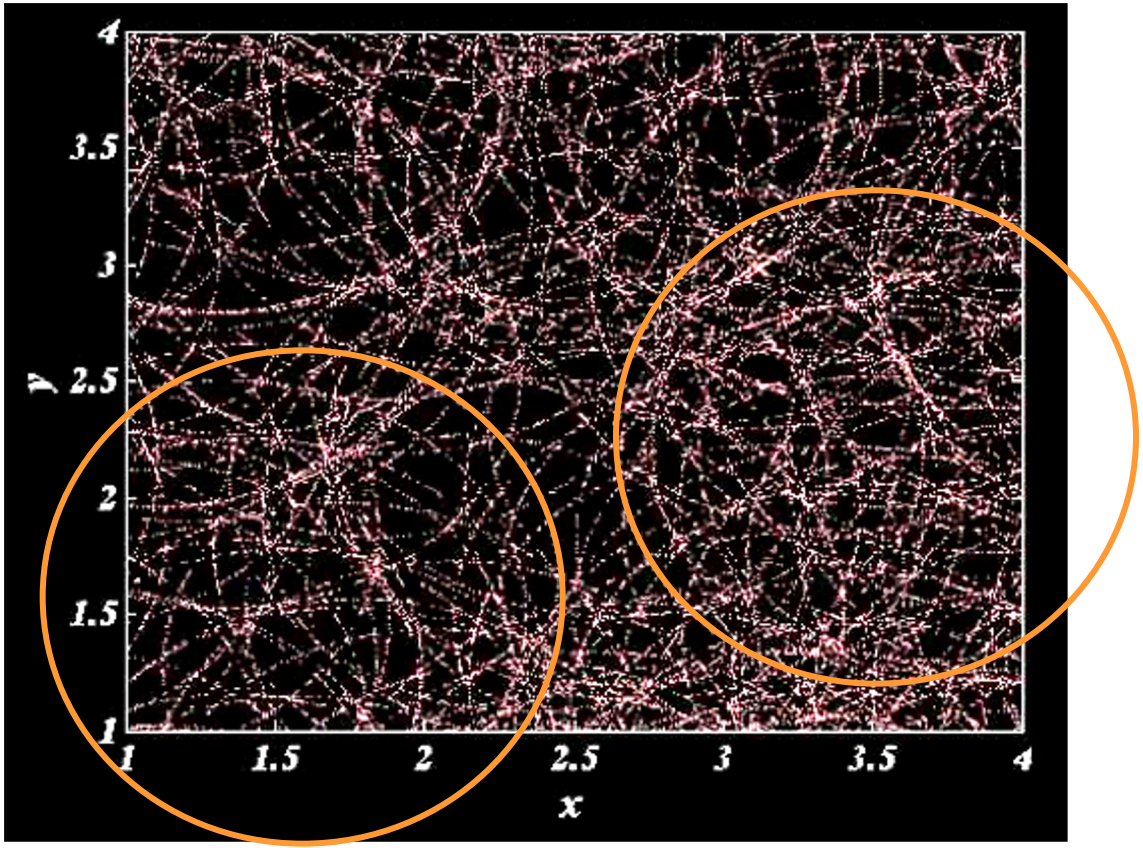


Rings of Power Superposed



Detecting the characteristic radius is now a statistical problem

Statistical Standard Rulers



Power Spectrum Errors

$$\frac{\delta P}{P} = \underbrace{\frac{1}{\sqrt{m}}}_{\text{Cosmic Variance}}\underbrace{\left(1 + \frac{1}{nP}\right)}_{\text{Shot Noise}}$$

m = number of Fourier modes measured in the survey
n = mean galaxy number density in the survey
P = P(k)

Bassett & Hlozek (2009)

BAO scale

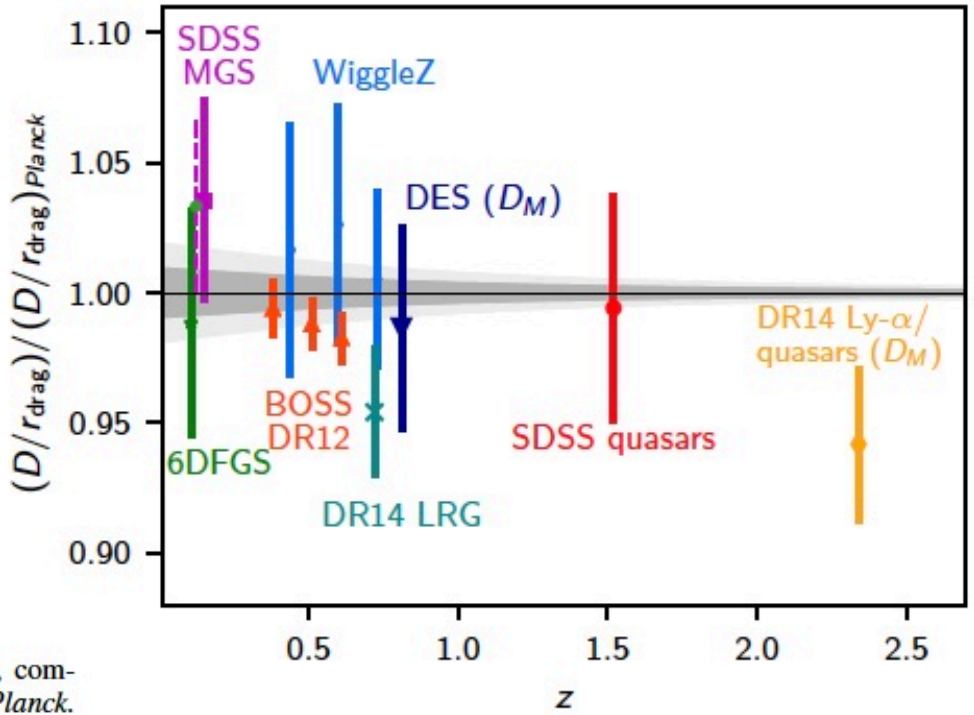


Fig. 27. Redshift-distance relation measured by BAO surveys, compared to the predictions of the ΛCDM model constrained by *Planck*. The grey band centred at unity shows the ±1 and ±2σ confidence regions for the *Planck* prediction, given the remaining uncertainties in the parameters. This is a percent-level prediction of the distance scale. The BAO points are: 6dFGS, green star (Beutler et al. 2011); SDSS MGS, purple square (Ross et al. 2015); BOSS DR12, red triangles (Alam et al. 2017); WiggleZ, blue circles (Kazin et al. 2014); SDSS quasars, red circle (Ata et al. 2018); and BOSS Ly α, yellow cross (Bautista et al. 2017).

Planck 2018 results (Overview)

C. A. Wuensche (2021)

Planck 2018 results

Table 2. Parameter 68% intervals for the base-ΛCDM model from *Planck* CMB power spectra, in combination with CMB lensing reconstruction and BAO.

Parameter	TT+lowE 68% limits	TE+lowE 68% limits	EE+lowE 68% limits	TT,TE,EE+lowE 68% limits	TT,TE,EE+lowE+lensing 68% limits	TT,TE,EE+lowE+lensing+BAO 68% limits
$\Omega_b h^2$	0.02212 ± 0.00022	0.02249 ± 0.00025	0.0240 ± 0.0012	0.02236 ± 0.00015	0.02237 ± 0.00015	0.02242 ± 0.00014
$\Omega_c h^2$	0.1206 ± 0.0021	0.1177 ± 0.0020	0.1158 ± 0.0046	0.1202 ± 0.0014	0.1200 ± 0.0012	0.11933 ± 0.00091
$100\theta_{MC}$	1.04077 ± 0.00047	1.04139 ± 0.00049	1.03999 ± 0.00089	1.04090 ± 0.00031	1.04092 ± 0.00031	1.04101 ± 0.00029
τ	0.0522 ± 0.0080	0.0496 ± 0.0085	0.0527 ± 0.0090	$0.0544^{+0.0070}_{-0.0081}$	0.0544 ± 0.0073	0.0561 ± 0.0071
$\ln(10^{10} A_s)$	3.040 ± 0.016	$3.018^{+0.020}_{-0.018}$	3.052 ± 0.022	3.045 ± 0.016	3.044 ± 0.014	3.047 ± 0.014
n_s	0.9626 ± 0.0057	0.967 ± 0.011	0.980 ± 0.015	0.9649 ± 0.0044	0.9649 ± 0.0042	0.9665 ± 0.0038
H_0 [km s^{-1} Mpc^{-1}]	66.88 ± 0.92	68.44 ± 0.91	69.9 ± 2.7	67.27 ± 0.60	67.36 ± 0.54	67.66 ± 0.42
Ω_Λ	0.679 ± 0.013	0.699 ± 0.012	$0.711^{+0.033}_{-0.026}$	0.6834 ± 0.0084	0.6847 ± 0.0073	0.6889 ± 0.0056
Ω_m	0.321 ± 0.013	0.301 ± 0.012	$0.289^{+0.026}_{-0.033}$	0.3166 ± 0.0084	0.3153 ± 0.0073	0.3111 ± 0.0056
$\Omega_m h^2$	0.1434 ± 0.0020	0.1408 ± 0.0019	$0.1404^{+0.0034}_{-0.0039}$	0.1432 ± 0.0013	0.1430 ± 0.0011	0.14240 ± 0.00087
$\Omega_m h^3$	0.09589 ± 0.00046	0.09635 ± 0.00051	$0.0981^{+0.0016}_{-0.0018}$	0.09633 ± 0.00029	0.09633 ± 0.00030	0.09635 ± 0.00030
σ_8	0.8118 ± 0.0089	0.793 ± 0.011	0.796 ± 0.018	0.8120 ± 0.0073	0.8111 ± 0.0060	0.8102 ± 0.0060
$S_8 \equiv \sigma_8 (\Omega_m/0.3)^{0.5}$	0.840 ± 0.024	0.794 ± 0.024	$0.781^{+0.052}_{-0.060}$	0.834 ± 0.016	0.832 ± 0.013	0.825 ± 0.011
$\sigma_8 \Omega_m^{0.25}$	0.611 ± 0.012	0.587 ± 0.012	0.583 ± 0.027	0.6090 ± 0.0081	0.6078 ± 0.0064	0.6051 ± 0.0058
z_{re}	7.50 ± 0.82	$7.11^{+0.91}_{-0.75}$	$7.10^{+0.87}_{-0.73}$	7.68 ± 0.79	7.67 ± 0.73	7.82 ± 0.71
$10^9 A_s$	2.092 ± 0.034	2.045 ± 0.041	2.116 ± 0.047	$2.101^{+0.031}_{-0.034}$	2.100 ± 0.030	2.105 ± 0.030
$10^9 A_s e^{-2\tau}$	1.884 ± 0.014	1.851 ± 0.018	1.904 ± 0.024	1.884 ± 0.012	1.883 ± 0.011	1.881 ± 0.010
Age [Gyr]	13.830 ± 0.037	13.761 ± 0.038	$13.64^{+0.16}_{-0.14}$	13.800 ± 0.024	13.797 ± 0.023	13.787 ± 0.020
z_*	1090.30 ± 0.41	1089.57 ± 0.42	$1087.8^{+1.6}_{-1.7}$	1089.95 ± 0.27	1089.92 ± 0.25	1089.80 ± 0.21
r_* [Mpc]	144.46 ± 0.48	144.95 ± 0.48	144.29 ± 0.64	144.39 ± 0.30	144.43 ± 0.26	144.57 ± 0.22
$100\theta_*$	1.04097 ± 0.00046	1.04156 ± 0.00049	1.04001 ± 0.00086	1.04109 ± 0.00030	1.04110 ± 0.00031	1.04119 ± 0.00029
z_{drag}	1059.39 ± 0.46	1060.03 ± 0.54	1063.2 ± 2.4	1059.93 ± 0.30	1059.94 ± 0.30	1060.01 ± 0.29
r_{drag} [Mpc]	147.21 ± 0.48	147.59 ± 0.49	146.46 ± 0.70	147.05 ± 0.30	147.09 ± 0.26	147.21 ± 0.23
k_D [Mpc^{-1}]	0.14054 ± 0.00052	0.14043 ± 0.00057	0.1426 ± 0.0012	0.14090 ± 0.00032	0.14087 ± 0.00030	0.14078 ± 0.00028
z_{eq}	3411 ± 48	3349 ± 46	3340^{+81}_{-92}	3407 ± 31	3402 ± 26	3387 ± 21
k_{eq} [Mpc^{-1}]	0.01041 ± 0.00014	0.01022 ± 0.00014	$0.01019^{+0.00025}_{-0.00028}$	0.010398 ± 0.000094	0.010384 ± 0.000081	0.010339 ± 0.000063
$100\theta_{s,eq}$	0.4483 ± 0.0046	0.4547 ± 0.0045	0.4562 ± 0.0092	0.4490 ± 0.0030	0.4494 ± 0.0026	0.4509 ± 0.0020
f_{2000}^{143}	31.2 ± 3.0			29.5 ± 2.7	29.6 ± 2.8	29.4 ± 2.7
$f_{2000}^{143\times217}$	33.6 ± 2.0			32.2 ± 1.9	32.3 ± 1.9	32.1 ± 1.9
f_{2000}^{217}	108.2 ± 1.9			107.0 ± 1.8	107.1 ± 1.8	106.9 ± 1.8

C. A. Wuensche (2021)

Why BAO in radio?

- Complementary to optics, different systematics
- Decay time of HI hyperfine transition is ~ 10^{15} seconds, but 75% of visible matter in the Universe is made of H...
- Efficient alternative for measuring a large number of galaxies individually (plus integrating the signal "alla" CMB allows for the reutilization of a large background experience in instrumentation and data analysis)
- Interferometers are excellent instruments for these measurements, but: more expensive, hard to operate and maintain
- Approach: single-dish, many horns X single horn per dish

TO BE CONTINUED:
THE BINGO RADIOTELESCOPE